NASA/TM—2014-217891 AIAA–2013–0027

Entry, Descent, and Landing with Propulsive Deceleration: Supersonic Retropropulsion Wind Tunnel Testing and Shock Phenomena

Bryan Palaszewski
Glenn Research Center, Cleveland, Ohio

September 2014

NASA STI Program . . . in Profile

Since its founding, NASA has been dedicated to the advancement of aeronautics and space science. The NASA Scientific and Technical Information (STI) program plays a key part in helping NASA maintain this important role.

The NASA STI Program operates under the auspices of the Agency Chief Information Officer. It collects, organizes, provides for archiving, and disseminates NASA's STI. The NASA STI program provides access to the NASA Aeronautics and Space Database and its public interface, the NASA Technical Reports Server, thus providing one of the largest collections of aeronautical and space science STI in the world. Results are published in both non-NASA channels and by NASA in the NASA STI Report Series, which includes the following report types:

- TECHNICAL PUBLICATION. Reports of completed research or a major significant phase of research that present the results of NASA programs and include extensive data or theoretical analysis. Includes compilations of significant scientific and technical data and information deemed to be of continuing reference value. NASA counterpart of peer-reviewed formal professional papers but has less stringent limitations on manuscript length and extent of graphic presentations.

- TECHNICAL MEMORANDUM. Scientific and technical findings that are preliminary or of specialized interest, e.g., quick release reports, working papers, and bibliographies that contain minimal annotation. Does not contain extensive analysis.

- CONTRACTOR REPORT. Scientific and technical findings by NASA-sponsored contractors and grantees.

- CONFERENCE PUBLICATION. Collected papers from scientific and technical conferences, symposia, seminars, or other meetings sponsored or cosponsored by NASA.

- SPECIAL PUBLICATION. Scientific, technical, or historical information from NASA programs, projects, and missions, often concerned with subjects having substantial public interest.

- TECHNICAL TRANSLATION. English-language translations of foreign scientific and technical material pertinent to NASA's mission.

Specialized services also include creating custom thesauri, building customized databases, organizing and publishing research results.

For more information about the NASA STI program, see the following:

- Access the NASA STI program home page at *http://www.sti.nasa.gov*

- E-mail your question to *help@sti.nasa.gov*

- Fax your question to the NASA STI Information Desk at 443–757–5803

- Phone the NASA STI Information Desk at 443–757–5802

- Write to:
  STI Information Desk
  NASA Center for AeroSpace Information
  7115 Standard Drive
  Hanover, MD 21076–1320

NASA/TM—2014-217891 AIAA–2013–0027

Entry, Descent, and Landing with Propulsive Deceleration: Supersonic Retropropulsion Wind Tunnel Testing and Shock Phenomena

Bryan Palaszewski
Glenn Research Center, Cleveland, Ohio

Prepared for the
51st Aerospace Sciences Meeting
sponsored by the American Institute of Aeronautics and Astronautics
Grapevine, Texas, January 7–10, 2013

National Aeronautics and
Space Administration

Glenn Research Center
Cleveland, Ohio 44135

September 2014

Acknowledgments

We would like to thank Bob McCluskey (NASA GRC), Steve Pesek (Jacobs Sverdrup, JSV), Barry Piendl (JSV), and Scott Smrdel (also of JSV). The team also included the test hardware design expertise of Jim Buckley (Arctic Slope Research Corporation, ASRC) and David Root (also of ASRC). Also many thanks go out to Tim Bencic (NASA GRC) for work in pressure and temperature sensitive paints and the NASA GRC Imaging Technology Team of Chris Lynch (Wyle Information Systems, LLC) and Quentin Schwinn (Wyle Information Systems, LLC) for their expertise with high speed video camera setup and video data capturing.

Level of Review: This material has been technically reviewed by technical management.

Available from

NASA Center for Aerospace Information
7115 Standard Drive
Hanover, MD 21076–1320

National Technical Information Service
5301 Shawnee Road
Alexandria, VA 22312

Available electronically at http://www.sti.nasa.gov

Entry, Descent, and Landing with Propulsive Deceleration: Supersonic Retropropulsion Wind Tunnel Testing and Shock Phenomena

Bryan Palaszewski
National Aeronautics and Space Administration
Glenn Research Center
Cleveland, Ohio 44135

Abstract

The future exploration of the Solar System will require innovations in transportation and the use of entry, descent, and landing (EDL) systems at many planetary landing sites. The cost of space missions has always been prohibitive, and using the natural planetary and planet's moon atmospheres for entry, and descent can reduce the cost, mass, and complexity of these missions. This paper will describe some of the EDL ideas for planetary entry and survey the overall technologies for EDL that may be attractive for future Solar System missions. Future EDL systems may include an inflatable decelerator for the initial atmospheric entry and an additional supersonic retropropulsion (SRP) rocket system for the final soft landing.

A three engine retropropulsion configuration with a 2.5 in. diameter sphere-cone aeroshell model was tested in the NASA Glenn Research Center's 1- by 1-ft (1×1) Supersonic Wind Tunnel (SWT). The testing was conducted to identify potential blockage issues in the tunnel, and visualize the rocket flow and shock interactions during supersonic and hypersonic entry conditions. Earlier experimental testing of a 70° Viking-like (sphere-cone) aeroshell was conducted as a baseline for testing of a SRP system. This baseline testing defined the flow field around the aeroshell and from this comparative baseline data, retropropulsion options will be assessed. Images and analyses from the SWT testing with 300- and 500-psia rocket engine chamber pressures are presented here. In addition, special topics of electromagnetic interference with retropropulsion induced shock waves and retropropulsion for Earth launched booster recovery are also addressed.

1.0 Introduction

Entry, descent, and landing (EDL) are a series of events needed to safely land on the surface of another body in the solar system which possesses an atmosphere. Thusly, Mars, Venus, the outer planets, and the outer planet moon, Titan, all require technologies that will protect the spacecraft from the high temperatures created during the initial hypersonic entry, and finally slow the vehicle from that hypersonic speed into the supersonic regime, then to subsonic and of course the final touchdown. In the outer planet atmospheres, the final landing would be replaced with a buoyancy system such as an airship or balloon, or an aircraft.

2.0 Historical Missions

Landing space vehicles on other planetary bodies is a challenge in propulsion, precision, control, and guidance. As there is no atmosphere surrounding Earth's Moon, the lunar landings of robotic Surveyor and human Apollo missions used propulsion for the entire descent. The same was true for the successful Luna and Lunakhod flights of the U.S.S.R. For Venus with its dense atmosphere, landing vehicles used aeroshell and parachute combinations, with crushable elements (balsa wood, etc.) to absorb the final landing energy. On Mars, the landing vehicles became more massive and complex (Viking, Pathfinder, Mars Exploration Rovers (MER), Mars Science Laboratory (MSL)), and the since the atmosphere was very thin, the final landing systems was a combination for aeroshell, parachute and retro rockets. To allow landing in more rugged areas of Mars, an additional airbag system was devised for the Pathfinder and MER landers to assure a successful landing in rock strewn sites.

3.0 Mars

Several EDL configurations are under assessment for Mars. Figure 1 presents the historical comparison of the U.S. Mars entry capsules (Ref. 1). The typical 70° cone angle for these configurations was selected for high stability and high drag. As the planet's atmosphere is quite thin, the blunt body can provide the needed drag for relatively small payloads of up 1 metric ton. As the mass of the lander vehicle increases, a different set of EDL technologies are required. Based on past studies (Refs. 2 and 3), parachutes are impractical for vehicles with lander masses of over 20 metric tons. The lander's parachutes would be too big to deploy effectively and reliably. Therefore a combination of inflatable decelerators (for hypersonic and supersonic speeds) and SRP has been suggested. Many past studies have investigated landing on Mars with aerodynamic systems (Ref. 4 to 8). However, the most recent studies imply that the past studies assumptions are too optimistic and are in need of revision to assure success. Supersonic retropropulsion, perhaps beginning as early as Mach 5, will therefore likely be required for soft landing on Mars.

4.0 Experimental Planning

While the Viking-like aeroshell design has proven successful for missions, but higher mass missions of many tens of tons will likely require more energetic retropropulsion. Figure 2 and Figure 3 show some of the historical testing on SRP (Ref. 3). This testing was only pursued with relatively small models and did not result in flight test hardware. To expand the relatively small data base of SRP information, a series of test programs were established and planned. The 1×1 SWT was used for the testing. It has a wide range of test velocities from Mach 2.0 to 6.0. Several types of data were gathered during the testing: surface pressure measurements, surface temperature measurements, and low speed and high speed digital Schlieren video movie imaging.

Model development began for a 2.5-in. diameter aeroshell. The 2.5-in. size was selected based on the previous wind tunnel testing of the aerodynamic blockage of the tunnel. The initial model was based on the 70° sphere-cone shape of the Viking entry capsule. It was attached to a sting-strut that was adjustable and can hold the model at a flexible angle of attack from 0° to 20° of angle of attack (AoA). The construction of the model and sting strut was stainless steel. The model was also instrumented with both temperature sensors and pressure transducers. There were three thermocouples and nine pressure ports on the windward side of aeroshell. There were three thermocouples and three pressure ports on leeward side of aeroshell. One additional thermocouple was placed near the trailing edge of the strut. High frequency pressure transducers (kulites) were used to measure the engine chamber pressures and tunnel wall pressures in three locations. Optical access to the test section allowed imaging with low speed and high speed Schlieren video movie recording. The high speed Schlieren recordings were made at 500 frames per second.

5.0 Test Data

Testing commenced on March 17, 2010, for a 1 day period. The tunnel operations were very smooth and in each test run, the tunnel pressure increased until the flow was started on the model and a stable bow shock was established. The tunnel pressure was then adjusted until the minimum pressure for tunnel operation was reached. Data was taken at this point, and then successive data points were taken at the remaining Mach numbers. Measurements were taken at Mach = 2.5, 3.0, 3.5, 4.0, and 5.0. Trailer-provided air was used for the simulated rocket engine flow. The rocket nozzle design was derived from Reference 9.

During the testing, it was noted that with the 2.5-in. model, an initial stable bow shock could be established at all Mach numbers. Based on previous testing, no unanticipated aerodynamic blockage occurred when the engines were not firing. When the rocket engines were firing, significant tunnel unstarts occurred in only several runs, and their occurrences are noted in Table I. The tunnel unstarts occurred with all of the 500 psia runs at M = 2.5 and 3.0 and with all of the 300 psia runs at M = 2.5. At all other conditions, excellent model performance was demonstrated with minimal wall interactions.

Figure 4 shows a typical Schlieren image for the baseline SWT testing three retropropulsion engines. The Mach number was 2.91 (M = 3.0 range). The angle of attack was 0°. Note that at M = 3.0, the bow shock has a small interaction with the tunnel walls in the image. Additional data was gathered at Mach Number = 3.5, 4.0, and 5.0, with the angle of attack at 0.0°, and these results are shown in Figure 4 to Figure 7, respectively. As the Mach number increases, there is less noticeable or no wall shock interaction in the images. On most runs, we are searching and striving to reach the lowest Reynolds number (Re)/foot and the lowest total pressure at each Mach number, so that we can more accurately simulate the Mars entry conditions. Higher values of Re/foot can represent other atmospheric entries into Earth, the outer planets, and Titan.

The location of the bow shock very close to the sphere-cone model was unforeseen. The rocket engines in past testing have used higher engine pressures of up to 1500 psia, and thus the bow shock is often far from the body, perhaps one to several entry vehicle diameters. The lower pressures used here were seen to penetrate the bow shock and that shock remained very near the entry body model. Such shock locations will have likely significant influence on vehicle heating due to shock impingement, etc.

An important parameter for the retropropulsion testing is the thrust coefficient. It is the ratio of the thrust of the vehicle to the drag of the vehicle and is computed with this equation (Ref. 3):

$$C_T = \frac{2}{\gamma_\infty M_\infty^{\,2}} \cdot \frac{Pe}{P_\infty} \frac{Ae}{A_B} \left(1 + \gamma_e M_e^{\,2}\right)$$

Where:

C_T	Thrust coefficient
γ_∞	Ratio of specific heats at infinity
M_∞	Mach Number at infinity
P_e	Pressure at nozzle exit
P_∞	Pressure at infinity (tunnel pressure)
A_e	Nozzle exit area
A_B	Test article projected area
γ_e	Ratio of specific heats at nozzle exit
M_e	Mach Number at nozzle exit

Figure 8 illustrates the thrust coefficient versus Mach number for four engine chamber pressures: 200, 300, 500, and 1500 psia. The engine expansion ratio is 10:1. For the test cases below 500 psia, the thrust coefficient is a maximum of 0.36, Only when the chamber pressure is near 1500 psia and near M = 2.0 will the thrust coefficient be equal to or greater than 1.0. Computations of the thrust coefficients at other planned expansion ratios (4:1, 20:1, and 50:1) show very similar results.

Testing with retrorocket configurations was planned to include flexible changes of the nozzle expansion ratio and the angle of attack. The overall design of a retropropulsion model is shown in Figure 9 to Figure 11. Three expansion rations of 10:1, 20:1 and 4:1 are shown, respectively. Appendix A shows the Schlieren images from the runs with a chamber pressure of 300 and 500 psia, at an angle of attack of 0.0°, 10.0° and 15.0° . Again, over the entire test program, rocket engine chamber pressures of 200, 300 and 500 psia were tested with the 10:1 rocket engine expansion ratio. Appendix B provides the test conditions for each run: tunnel total and static pressures, and the tunnel Re/foot. Appendix C provides a detailed drawing of the windward side of the aeroshell test model.

6.0 Thoughts on Alternate Retropropulsion Configurations

Figure 12 shows the Mars Lander configuration of the Design Reference Architecture 5 (DRA-5, Ref. 8). As currently designed, the vehicle has a large series of open trusses that support the subsystems of the vehicle: tankage, propellants, engines, rover(s), return vehicle, etc. During EDL, it has been suggested that the aeroshell surrounding the vehicle can be released at supersonic speed and the main engines be used for SRP. With all of the major open trusses of the lander structure in the aerodynamics stream, this would lead to severe damage to the lander (and is not recommended). By using a combination of deployable structures and SRP, the vehicle could be much more controllable and safe from unwanted aerodynamic heating.

Saturn I retrorocket separation—The Saturn I rocket from the 1960s used a retrorocket system to assist with the first and second stage separation. The separation motors were solid rockets, and were used to assure that the stages did not collide during separation. The retro rocket flow field was analyzed (see Figure 13 and Figure 14) and predictions made of the influence of the flow field on vehicle communications (Ref. 10). Such analyses will likely be important in future Mars exploration missions using SRP.

U.S. Air Force (USAF) reusable booster system (RBS) Rocketback maneuver—The USAF RBS has been suggested as a potential new launch vehicle (Refs. 11 and 12). The RBS is composed on a reusable rocket powered first stage and a rocket powered second stage, as shown in Figure 15. In the suggested design, the booster staging separation velocity is so high that the first stage must employ a rocket back maneuver (see Figure 15). After staging, the first stage vehicle will turn to fire its main engines into the oncoming airflow, and slow the vehicle down so that it may return to the launch site. Figure 16 shows a flowfield calculation for 4 angles of attack (Ref. 12). Severe heating may be experienced during this maneuver.

Fins—Due to the severity and large variations of the flow field from the retro rockets, extensions from the entry body may be an important option for stability enhancements. Past testing at supersonic speed of fin extensions (grid fins, etc.) shows that such configurations can provide the stability enhancements for missiles and human rated vehicles (Russian Soyuz launch vehicle, etc.). The 4 grid fins are mounted on the sides of the vehicles and provide enhanced stability during the use of the launch escape system. U.S. Army and international missile testing (Refs. 13 to 23) has also evaluated grid fins. The missile testing was for long slender missiles, and hence the application may be for a more restricted set of higher lift to drag (L/D) EDL configurations (biconic aeroshells, etc.)

7.0 Concluding Remarks

Experimental programs were planned and executed to gather data of supersonic propulsive deceleration (or SRP). Initial data gathering was successful and this data will be used as the comparative baseline for upcoming larger scale retropropulsion testing. Schlieren imaging was captured to assess the successful formation of the bow shock surrounding the aeroshell. In some cases, the shock interactions with the SWT walls occurred and were also visualized. The high speed camera video at 500 frames per second identified the chaotic nature of the retrorocket—shock interactions. More detailed data and image analyses are continuing. Test planning and model development has been conducted for additional retrorocket equipped aeroshells with different area ratio rocket nozzles: 4:1, 20:1, and 50:1. Due to test time limitations, the 4:1, 20:1, and 50:1 expansion ratios were not tested.

Entry, descent, and landing (EDL) technologies are under development for the high mass Mars Entry system (HMMES). Many investigations of aerodynamic deceleration for the outer planets have been conducted as well. The challenges for EDL are numerous, especially for inflatable decelerator and the interactions that will occur with propulsive deceleration retro propulsion. The high velocities involved in entry and descent will require high temperature materials that are flexible for folding into a small volume, but reliable when they are deployed to their full diameter.

Many exciting possibilities are foreseen for Mars and outer planet exploration and exploitation (Refs. 24 to 40). The resources of the outer planets may allow fueling of nuclear fusion vehicles and other power plants that may be the engine for all of Earth's energy. Wresting fuels such as hydrogen and helium 3 from the gas giant planets may be a critical element of outer planet exploration and also flight to the nearby stars. The EDL systems will be an integral part of all of these exploration and exploitation scenarios.

TABLE I.—OVERALL RESULTS OF AND COMMENTS ON EDL SRP TEST MATRIX
[A 2.5-in.-diameter aeroshell model, three engine configuration. NASA EDL SRP 1×1 SWT test results summary, March 17, 2010]

Reading	Mach no.	AoA, deg.	P_{jet}, psia	Comment	Specifics
6	2.5	0	200	Some strong wall interaction	Some strong wall interactions interaction
9	2.5	0	300	Tunnel unstart, with recovery	Post firing: this firing is a potential unstart, with the tunnel taking *a few seconds* to recover the full Mach number after the engines are turned off.
10	2.5	0	500	Tunnel unstart, with recovery	Post firing: this firing is a potential unstart, with the tunnel recovering the full Mach number flow after the engines are turned off.
7	2.5	10	200	Some strong wall interaction	Some strong wall interaction
8	2.5	10	300	Tunnel unstart, with recovery	Post firing: this firing is a potential unstart, with the tunnel recovering the full Mach number flow after the engines are turned off.
11	2.5	10	500	Tunnel unstart, with recovery	Post firing: this firing is a potential unstart, with the tunnel recovering the full Mach number flow after the engines are turned off.
19	3.0	0	200	Spectacular	Minor wall interactions
20	3.0	0	300	Spectacular	Some strong wall interactions
23	3.0	0	500	Tunnel unstart, with recovery	Post firing: this firing is a potential unstart, with the tunnel recovering the full Mach number flow after the engines are turned off.
16A, 17	3.0	10	200	Spectacular	Minor wall interactions
21	3.0	10	300	Spectacular	Minor wall interactions
22	3.0	10	500	Tunnel unstart, with recovery	Post firing: this firing is a potential unstart, with the tunnel recovering the full Mach number flow after the engines are turned off.
24	3.0	15	500	Tunnel unstart, with recovery	Post firing: this firing is a potential unstart, with the tunnel recovering the full Mach number flow after the engines are turned off.
30	3.5	0	200	Spectacular	No wall interactions
35	3.5	0	300	Spectacular	No wall interactions
39	3.5	0	500	Spectacular	No wall interactions*
31	3.5	10	200	Spectacular	No wall interactions
34	3.5	10	300	Spectacular	No wall interactions
38	3.5	10	500	Spectacular	No wall interactions*
No rdg.	3.5	15	200	No data point taken	No data point taken
36	3.5	15	300	Spectacular	No wall interactions
37	3.5	15	500	Spectacular	No wall interactions*
43	4.0	0	200	Spectacular	No wall interactions
48	4.0	0	300	Spectacular	Some wall interactions
49	4.0	0	500	Spectacular	Minor wall interactions
44	4.0	10	200	Spectacular	Minor wall interactions, far downstream
47	4.0	10	300	Spectacular	No wall interactions
50	4.0	10	500	Spectacular	Minor wall interactions
45	4.0	15	200	Spectacular	Minor wall interactions, far downstream
46	4.0	15	300	Spectacular	Minor wall interactions, far downstream
51	4.0	15	500	Spectacular	Minor wall interactions, downstream, near backshell
63	5.0	0	200	Spectacular	No wall interactions. Required heater usage, T= 300 °F to establish stable shock on the model. Heater used in all M = 5.0 tests
64	5.0	0	300	Spectacular	No wall interactions
65	5.0	0	500	Spectacular	Minor wall interactions
62	5.0	10	200	Spectacular	No wall interactions
61	5.0	10	300	Spectacular	No wall interactions
60	5.0	10	500	Spectacular	No wall interactions
57	5.0	15	200	Spectacular	No wall interactions
58	5.0	15	300	Spectacular	No wall interactions
59	5.0	15	500	Spectacular	No wall interactions

	Viking 1/2	Pathfinder	MER A/B	Phoenix	MSL
	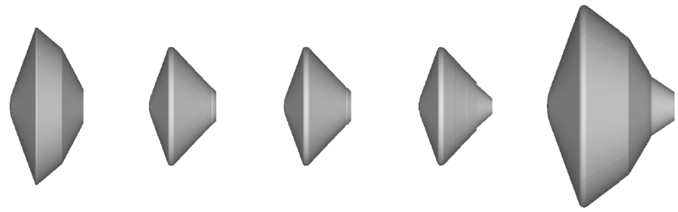				
Diameter, m	3.5	2.65	2.65	2.65	4.5
Entry Mass (kg)	930	585	840	602	> 3000
Landed Mass (kg)	603	360	539	364	> 1700
Landing Altitude (km)	-3.5	-1.5	-1.3	-3.5	< 1.0
Landing Ellipse (km)	420 x 200	100 x 50	80 x 20	75 x 20	< 10 x 10
Relative Entry Velocity (km/s)	4.5/4.42	7.6	5.5	5.9	> 5.5
Relative Entry FPA (deg)	-17.6	-13.8	-11.5	-13	-15.2
$m/(C_D S_{ref})$ (kg/m^2)	64	62	90	65	> 140
Turbulent at Peak Heating?	No	No	No	No	Yes
Peak Heat Flux (W/cm^2)	24	115	54	56	> 200
Peak Surface Pressure (atm)	0.10	0.20	0.10	0.12	> 0.3
Heatshield TPS Material	SLA-561V	SLA-561V	SLA-561V	SLA-561V	SLA-561V
Backshell TPS Material	None	SLA-561S	SLA-561S	SLA-561S	SLA-561V
Hypersonic α (deg)	-11	0	0	0	-16
Hypersonic L/D	0.18	0	0	0	0.24
Control	3-axis	Spinning	Spinning	3-axis	3-axis
Guidance	No	No	No	No	Yes

Figure 1.—Comparison of Viking-spacecraft-like (sphere-cone) aeroshells for Mars entry (Ref. 1).

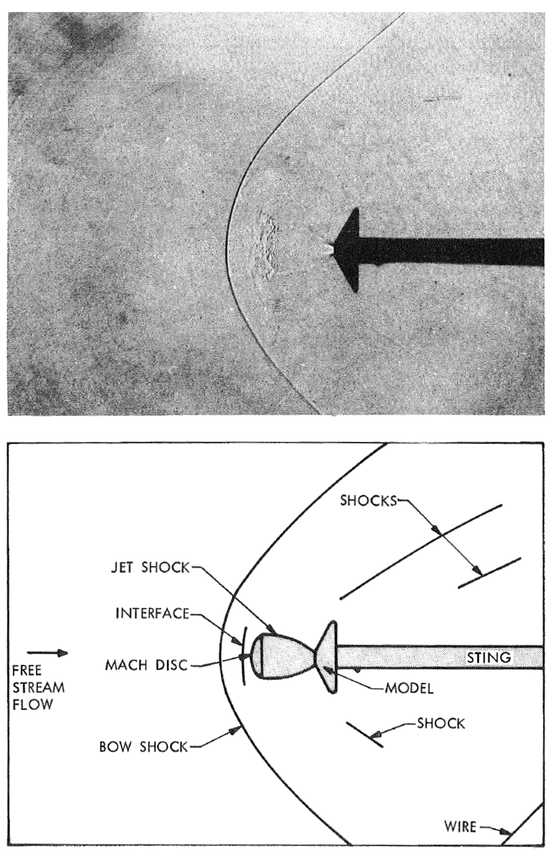

Single nozzle 60° aeroshell model with blunt flow interaction, M_∞ = 2.0, C_T = 1.1.

Figure 2.—Historical retropropulsion testing (Ref. 3, 1970).

Figure 3.—Historical retropropulsion testing, three engine configuration (Ref. 3, 1970).

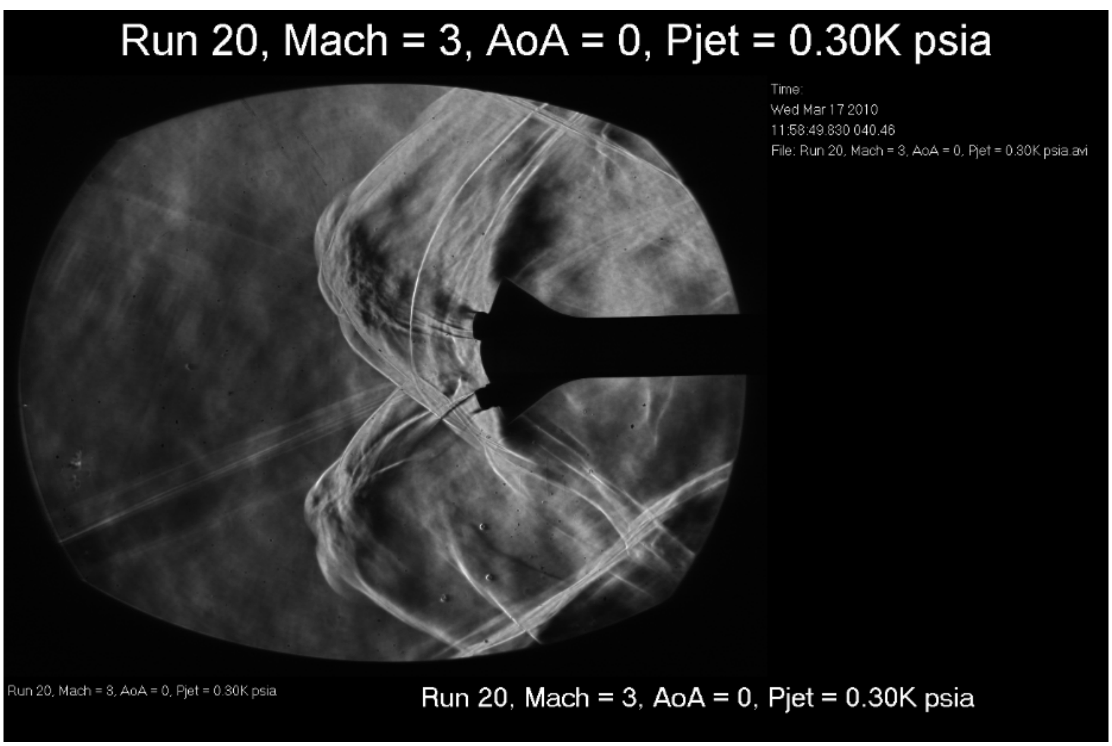

Figure 4.—Schlieren image from 1x1 SWT testing—three engine model, Mach = 3.0, Re/ft = 1.45×10^6, and P_{total} (psi) = 8.67, AoA = 0°, 300 psia engine chamber pressure.

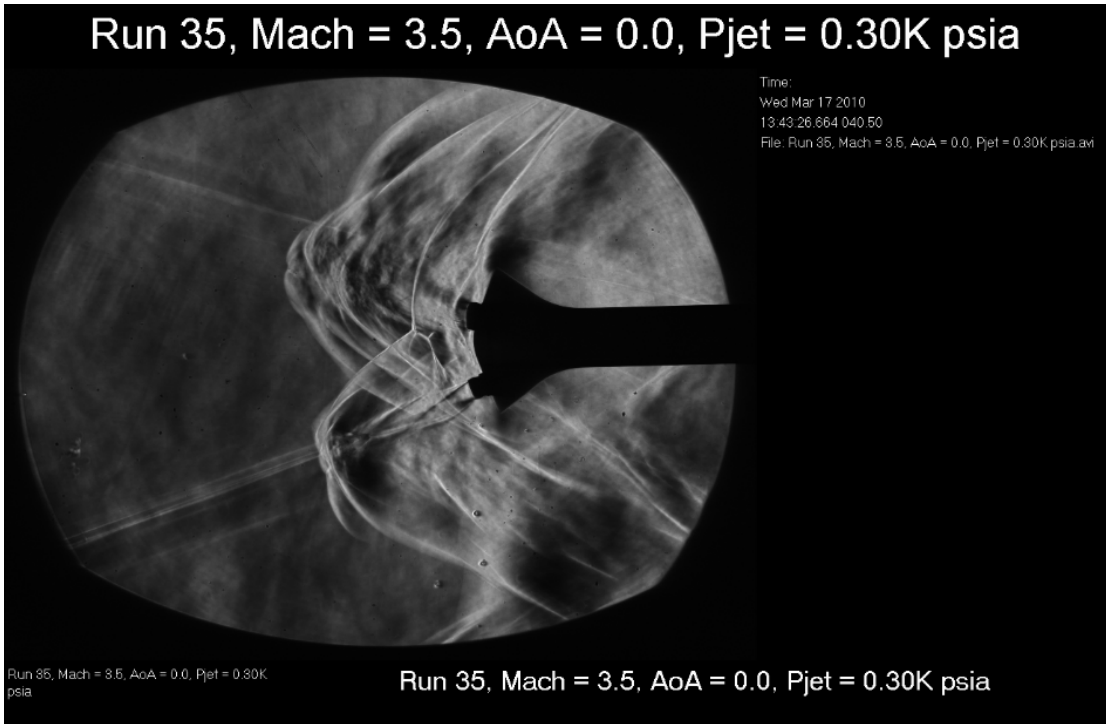

Figure 5.—Schlieren image from 1x1 SWT testing—three engine model, Mach = 3.5, Re/ft = $1.86\text{x}10^6$, and P_{total} (psi) = 15.00, AoA = 0°, 300 psia engine chamber pressure.

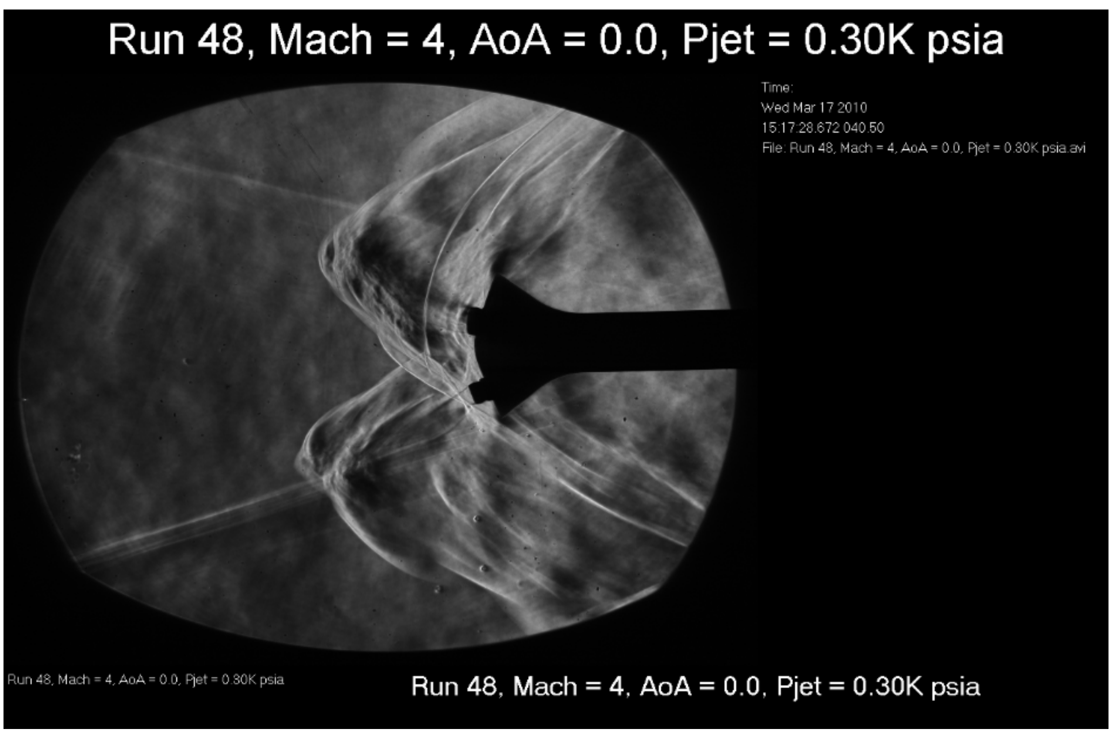

Figure 6.—Schlieren image from 1x1 SWT testing—three engine model, Mach = 4.0, Re/ft = $2.58\text{x}10^6$, and P_{total} (psi) = 26.13, AoA = 0°, 300 psia engine chamber pressure.

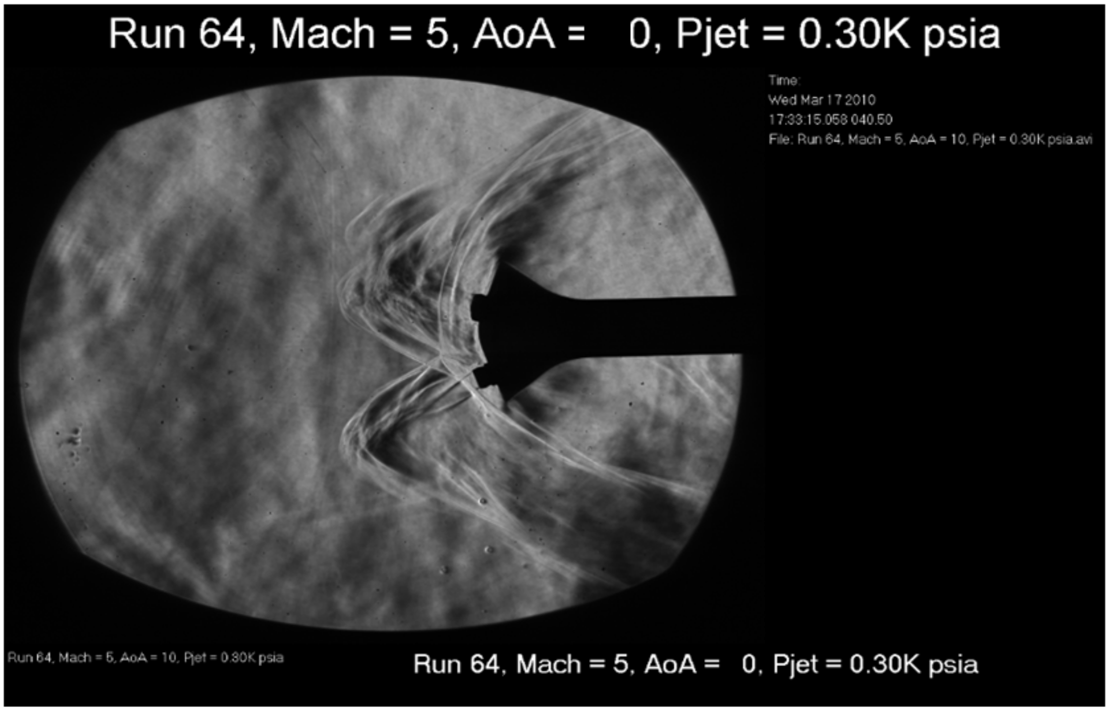

Figure 7.—Schlieren image from 1x1 SWT testing—three engine model, Mach = 5.0, Re/ft = 5.19x10^6, and P_{total} (psi) = 92.39, AoA = 0°, 300 psia engine chamber pressure.

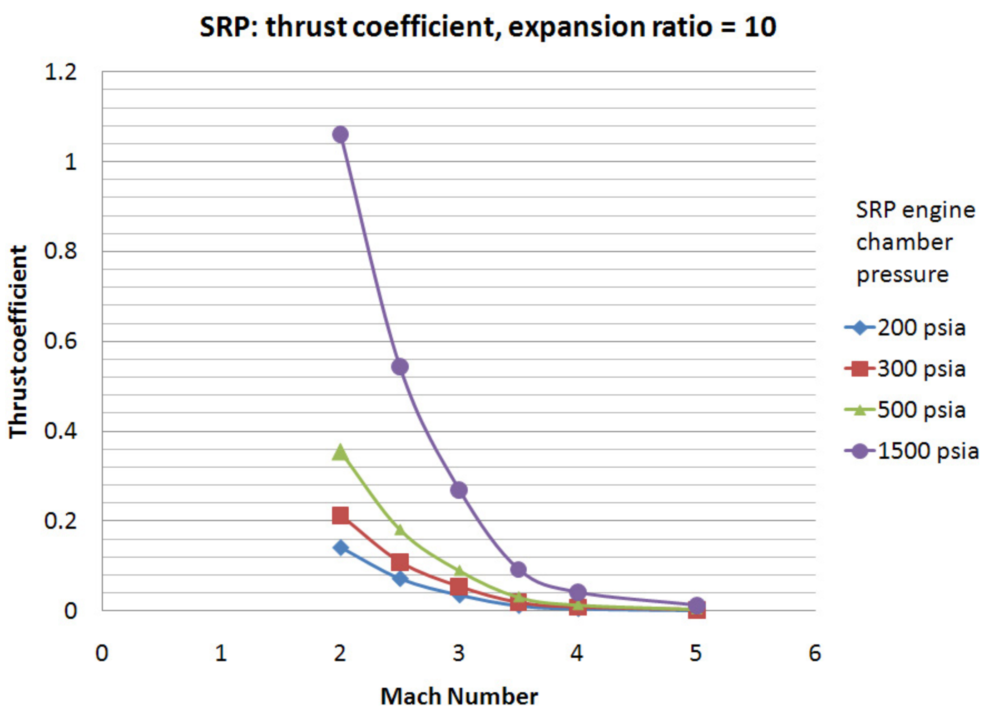

Figure 8.—Thrust coefficient versus Mach number for varying engine chamber pressures.

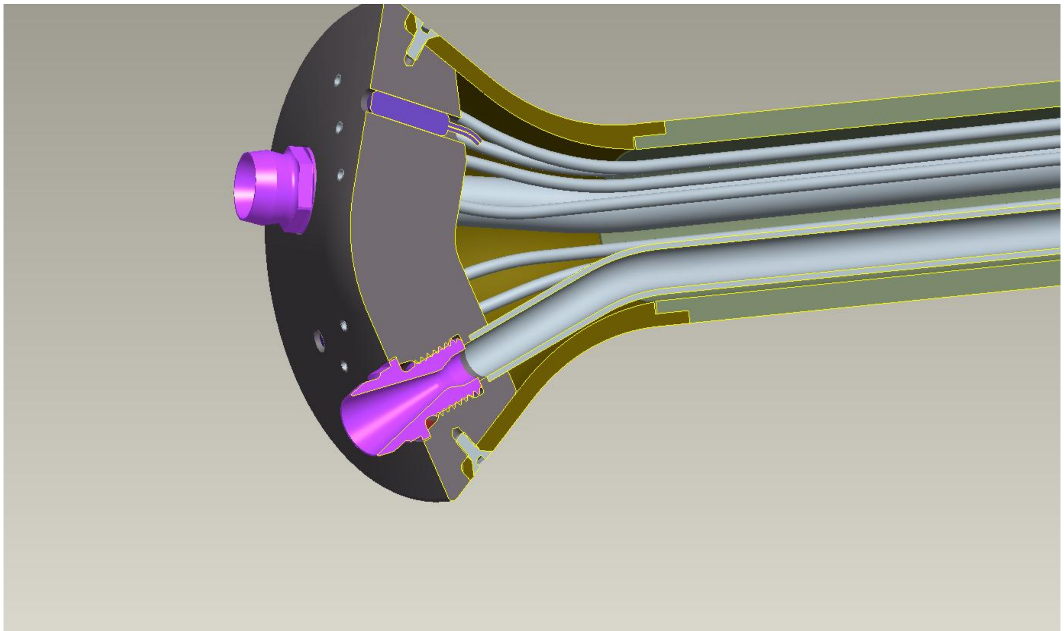

Figure 9.—Retropropulsion model for three engine configuration, with nozzle extensions (expansion ratio = 10:1).

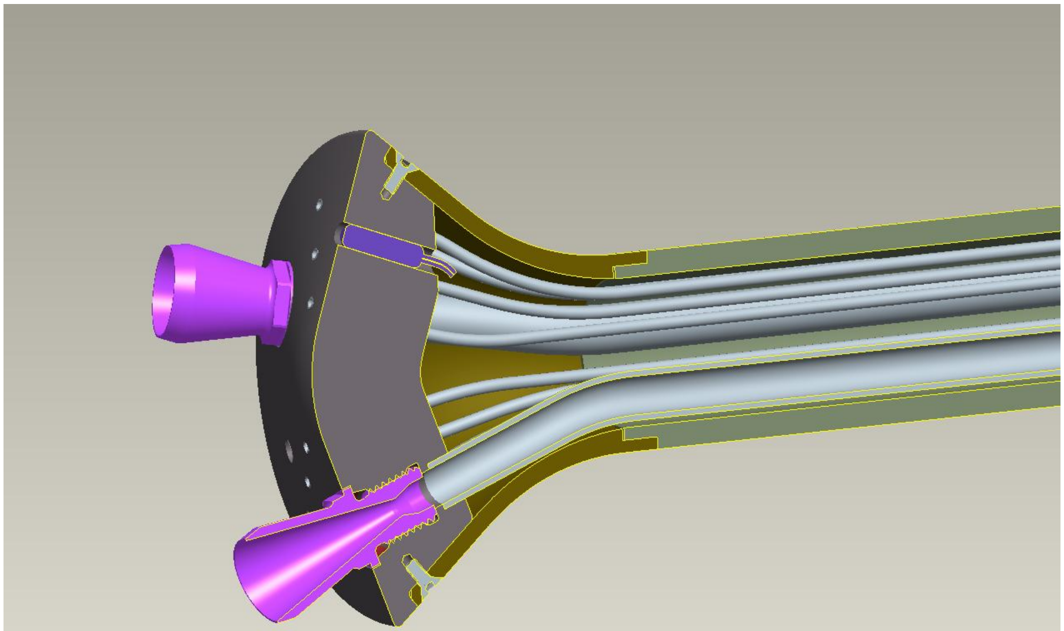

Figure 10.—Retropropulsion model for three engine configuration, with nozzle extensions (expansion ratio = 20:1).

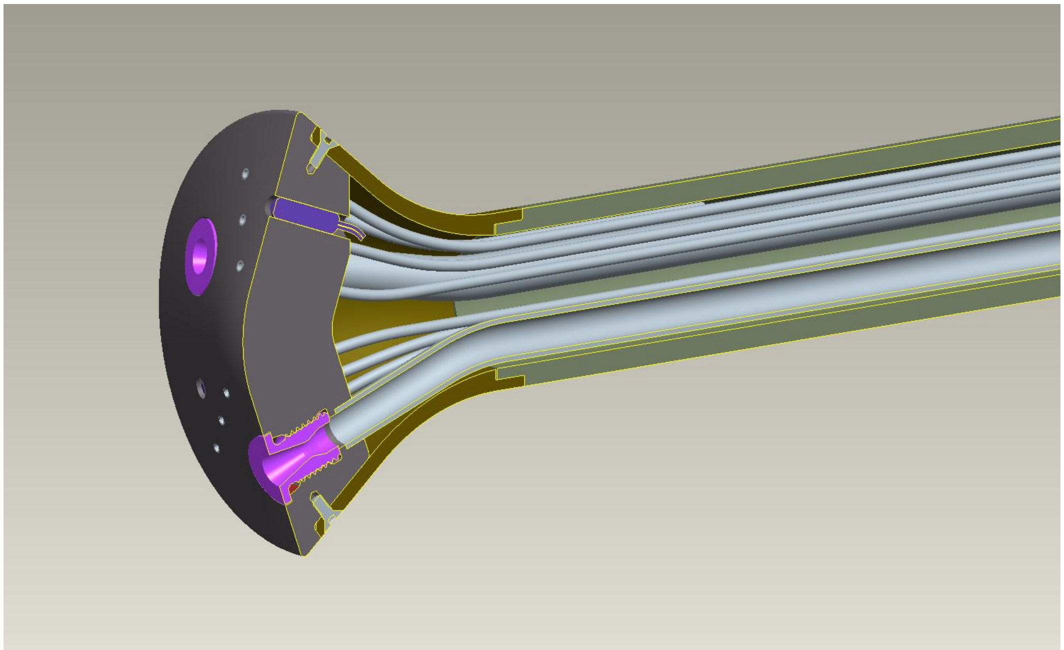

Figure 11.—Retropropulsion model for three engine configuration, with no nozzle extensions (expansion ratio = 4:1).

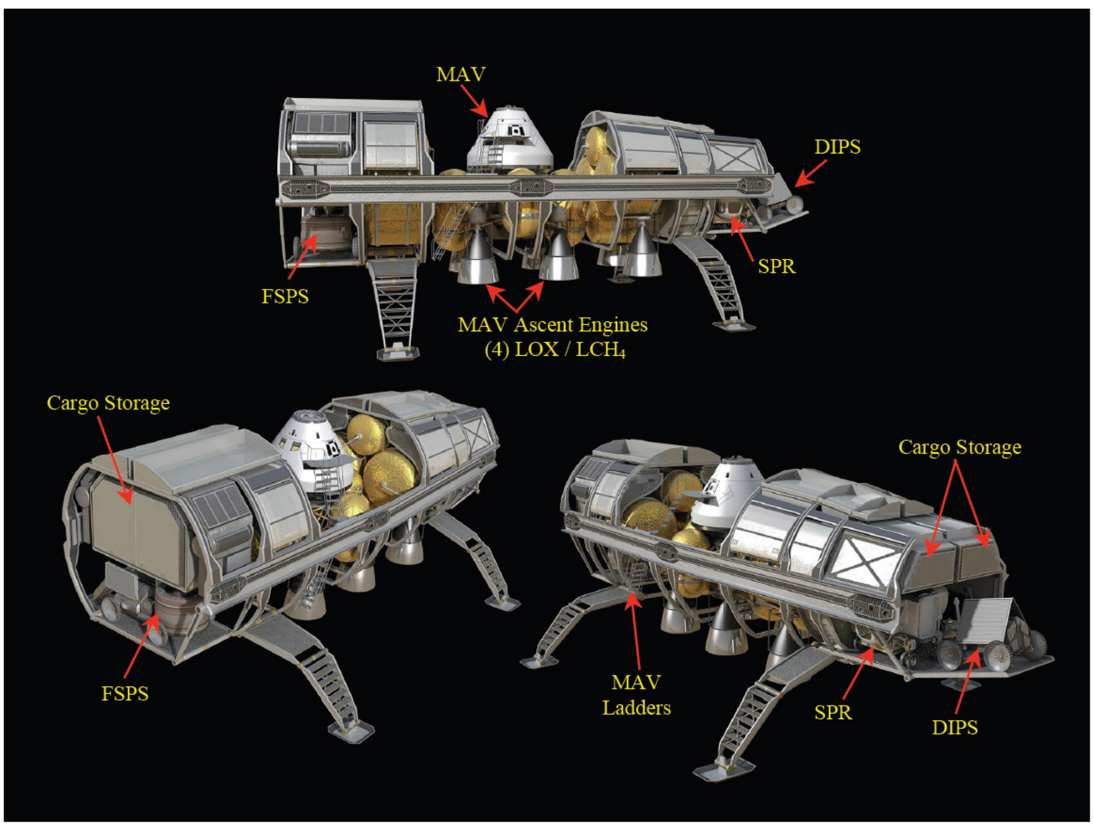

Figure 12.—Mars Lander Configuration, NASA DRA-5 (Ref. 8).

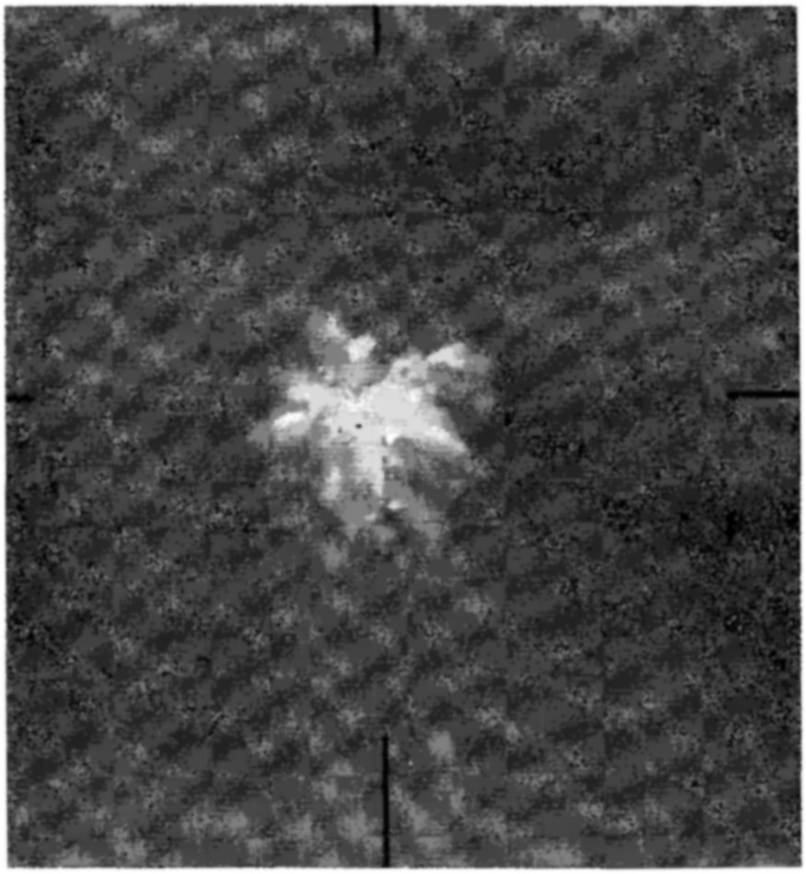

Figure 13.—Retrorocket plume at ignition.

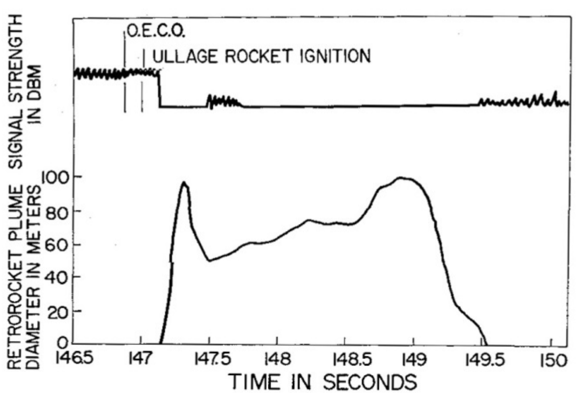

Figure 14.—Comparison of retrorocket plum size and telemetry signal strenght SA-5.

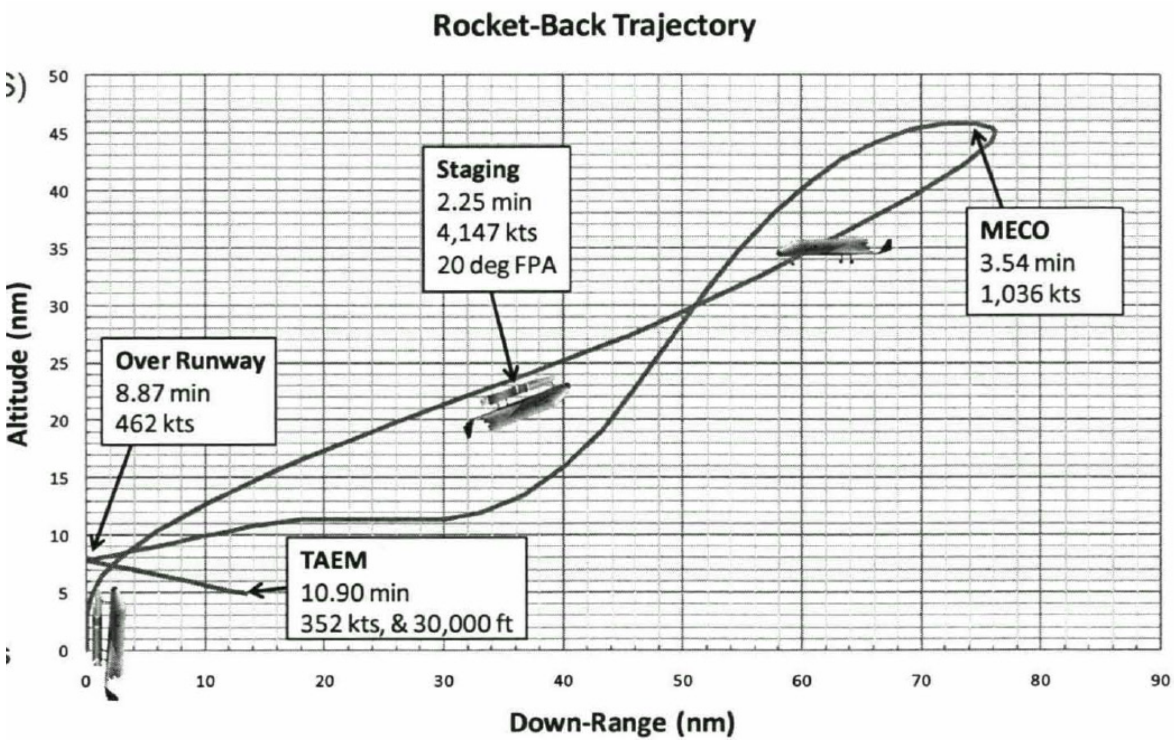

Figure 15.—Reusable Booster System Flight Path with Rocket Back Maneuver (Ref. 11).

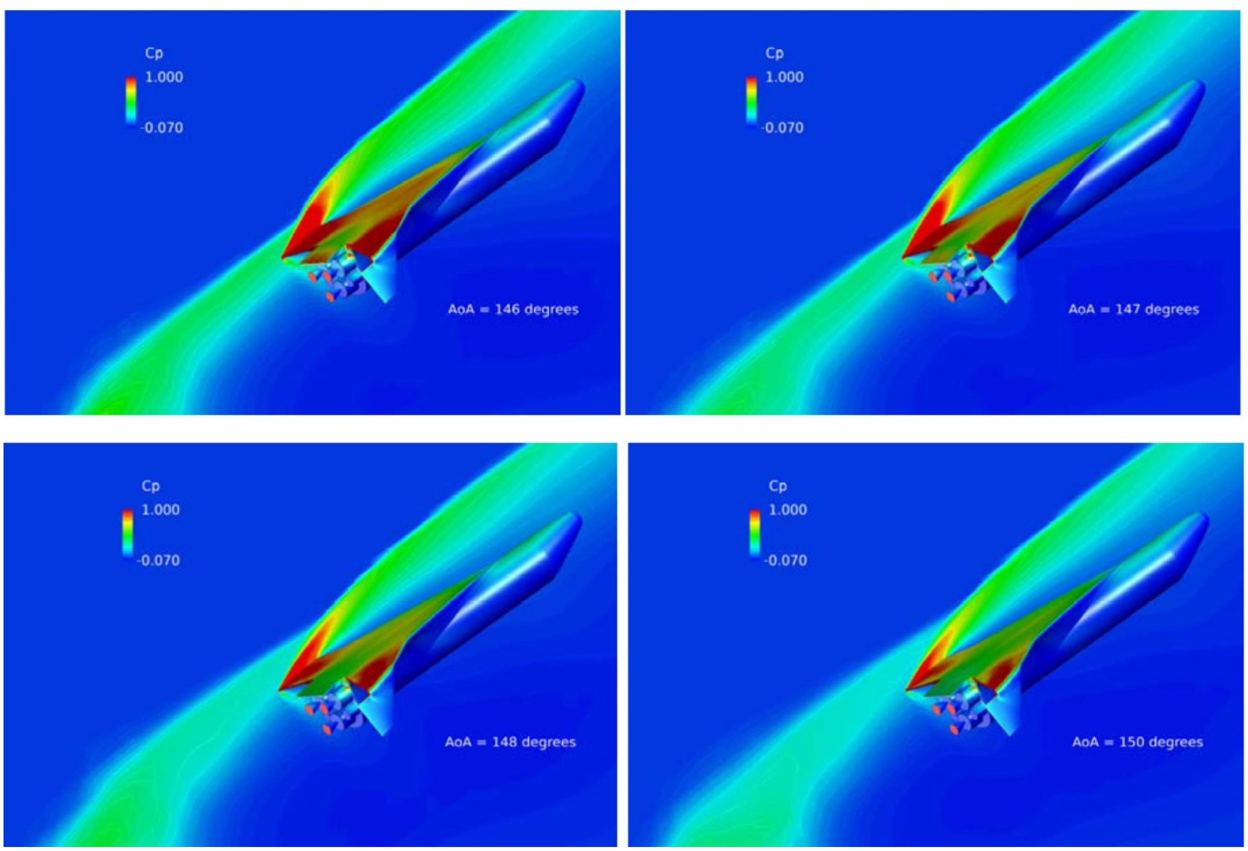

Steady-state C_p values on vehicle and off-body mid-span plane for four angles of attack, M = 4.5, Q = psf

Figure 16.—Reusable Booster System Cp Predictions for 4 Angles of Attack (Ref. 12)

Appendix A.—Schlieren Images

A.1 AoA = 10° (15°, in Some Cases), 300 psia Chamber Pressure

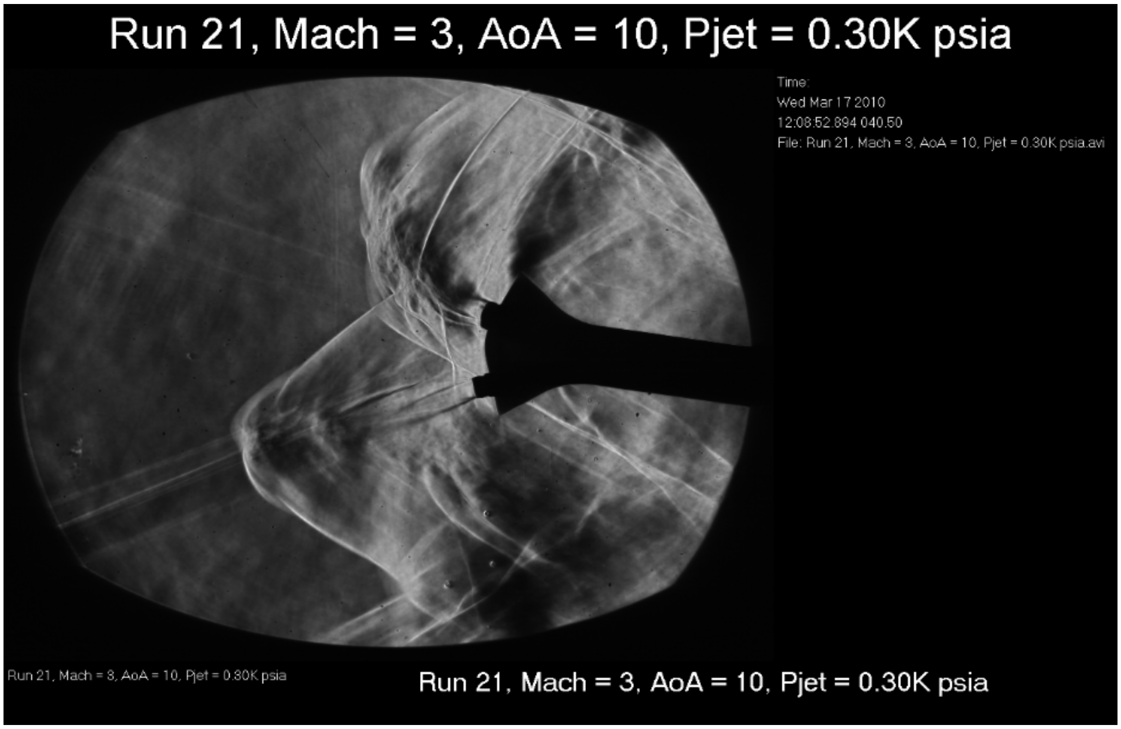

Figure A.1.—Schlieren image from 1x1 SWT testing—three engine model, Mach = 3.0, Re/ft = 1.42×10^6, and P_{total} (psi) = 8.49, AoA = 10°, 300 psia engine chamber pressure.

Figure A.2.—Schlieren image from 1x1 SWT testing—three engine model, Mach = 3.5, Re/ft = 1.87×10^6, and P_{total} (psi) = 15.03, AoA = 15°, 300 psia engine chamber pressure.

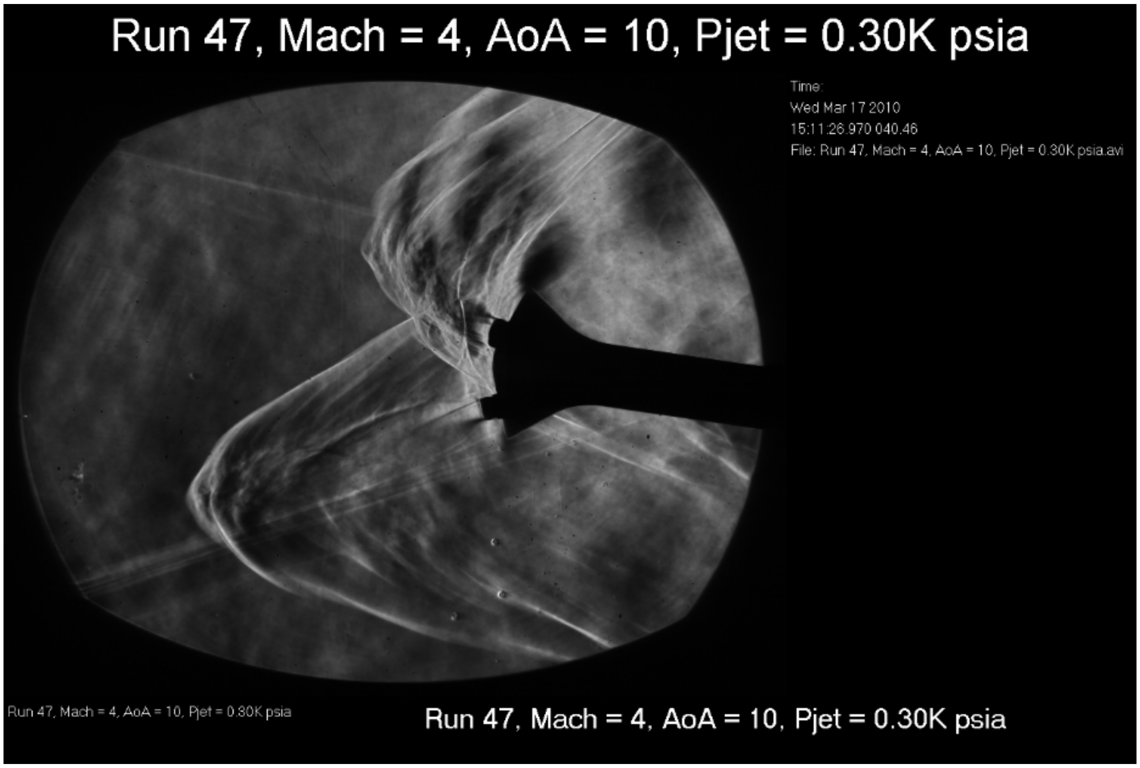

Figure A.3.—Schlieren image from 1x1 SWT testing—three engine model, Mach = 4.0, Re/ft = 2.57x10^{6}, and P_{total} (psi) = 25.94, AoA = 10°, 300 psia engine chamber pressure.

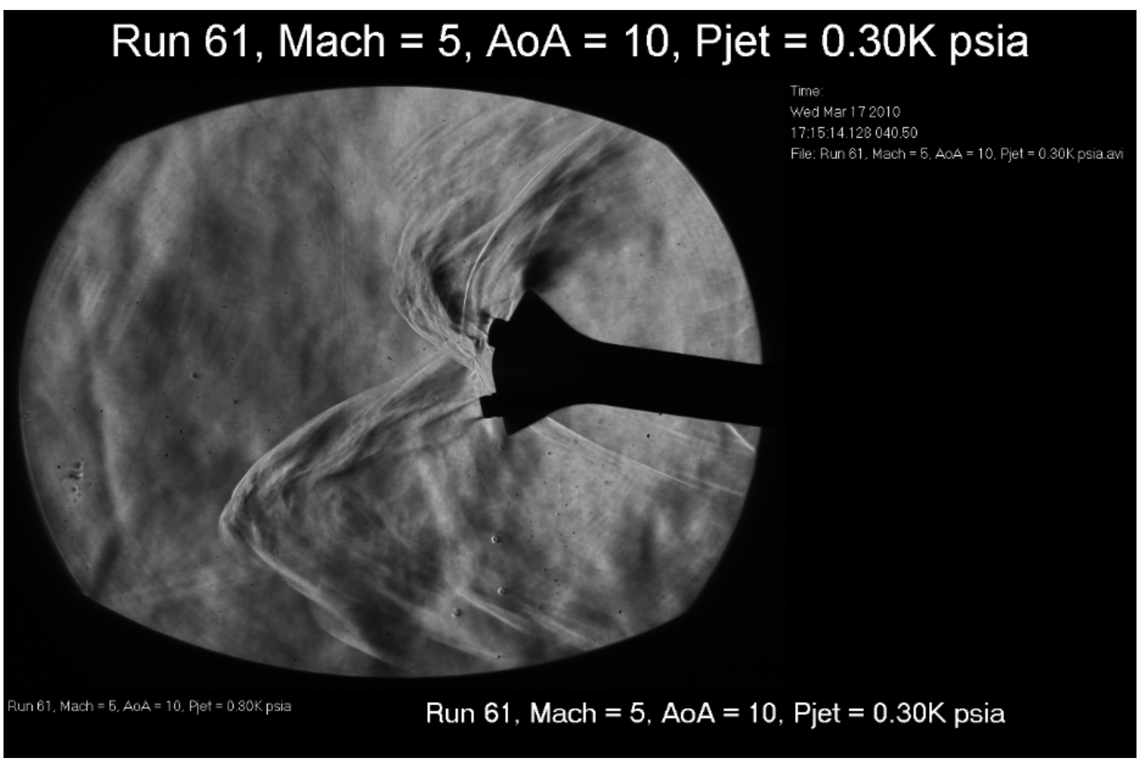

Figure A.4.—Schlieren image from 1x1 SWT testing—three engine model, Mach = 5.0, Re/ft = 5.32x10^{6}, and P_{total} (psi) = 90.37, AoA = 10°, 300 psia engine chamber pressure.

A.2 AoA = 0°, 500 psia Chamber Pressure

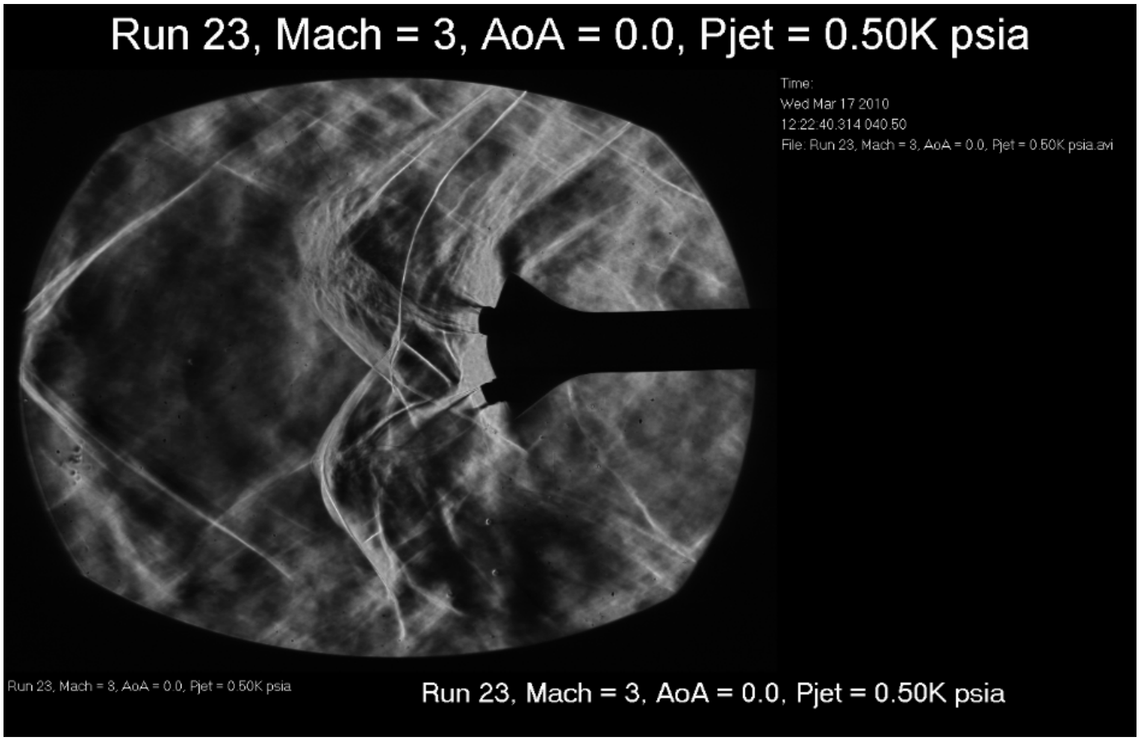

Figure A.5.—Schlieren image from 1x1 SWT testing—three engine model, Mach = 3.0, Re/ft = 1.50×10^6, and P_{total} (psi) = 8.95, AoA = 0°, 500 psia engine chamber pressure, tunnel unstart.

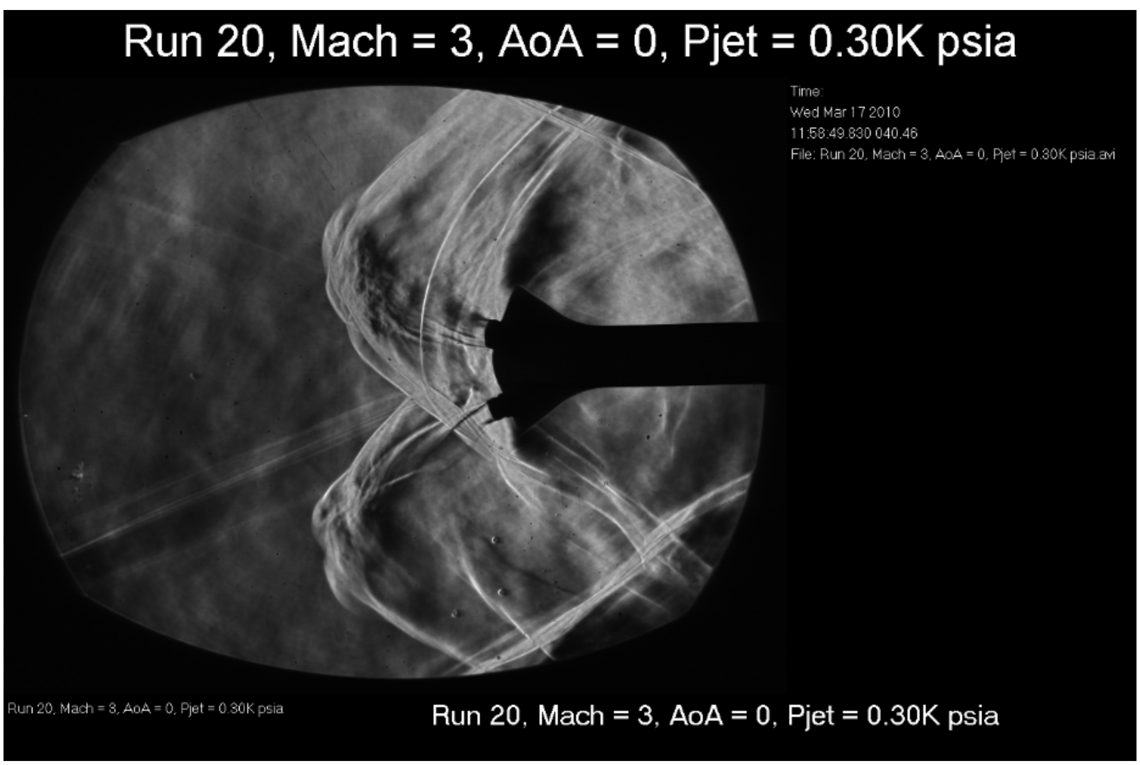

Figure A.6.—Schlieren image from 1x1 SWT testing—three engine model, Mach = 3.0, Re/ft = 1.45×10^6, and P_{total} (psi) = 8.67, AoA = 0°, 300 psia engine chamber pressure.

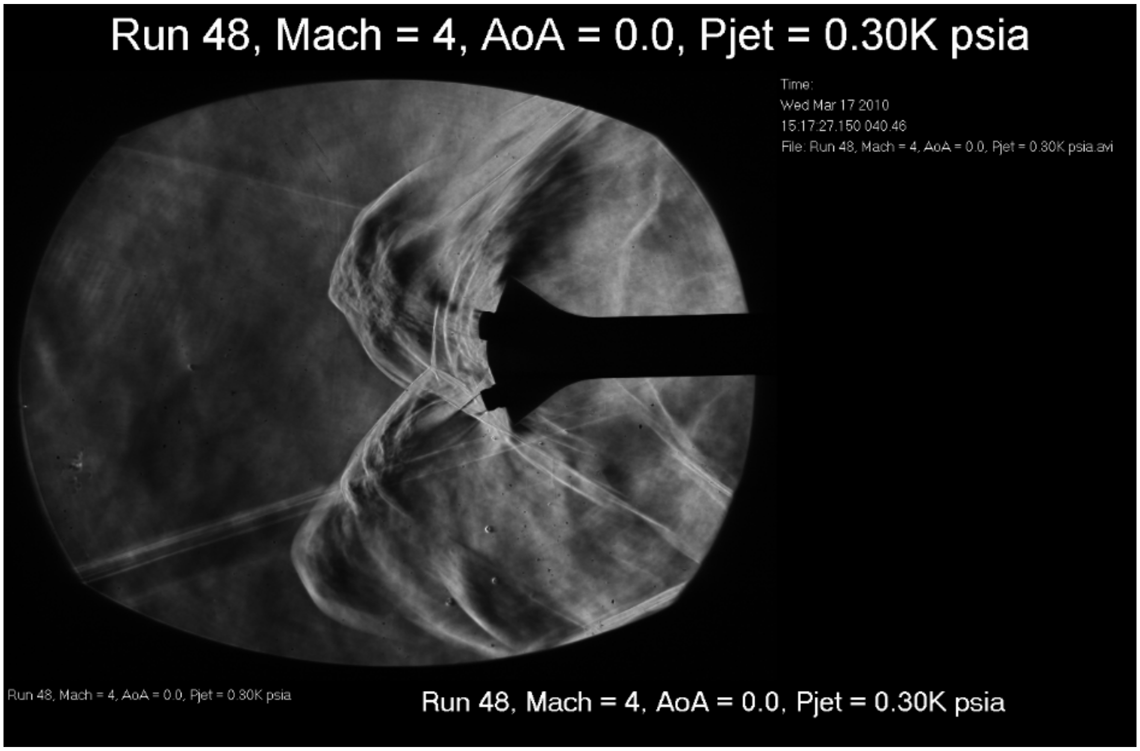

Figure A.7.—Schlieren image from 1x1 SWT testing—three engine model, Mach = 4.0, Re/ft = 2.60x10^6, and P_{total} (psi) = 26.33, AoA = 0°, 300 psia engine chamber pressure.

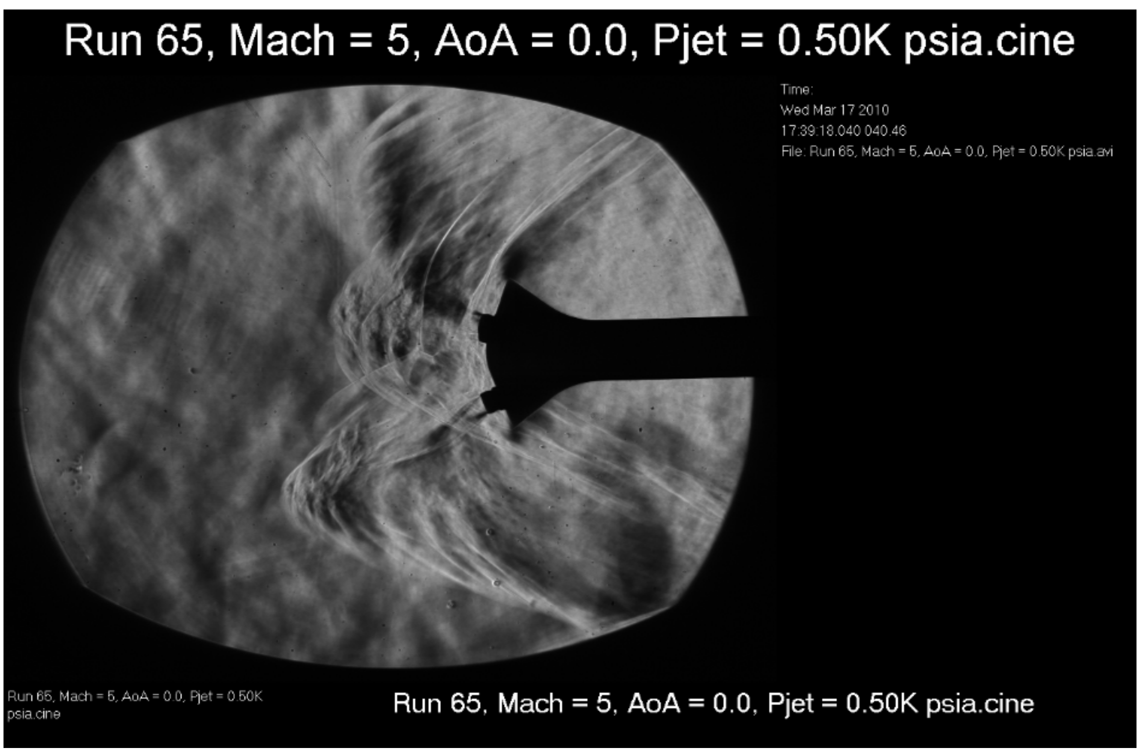

Figure A.8.—Schlieren image from 1x1 SWT testing—three engine model, Mach = 5.0, Re/ft = 4.91x10^6, and P_{total} (psi) = 89.36, AoA = 0°, 500 psia engine chamber pressure.

A.3 AoA = 10°, 500 psia Chamber Pressure

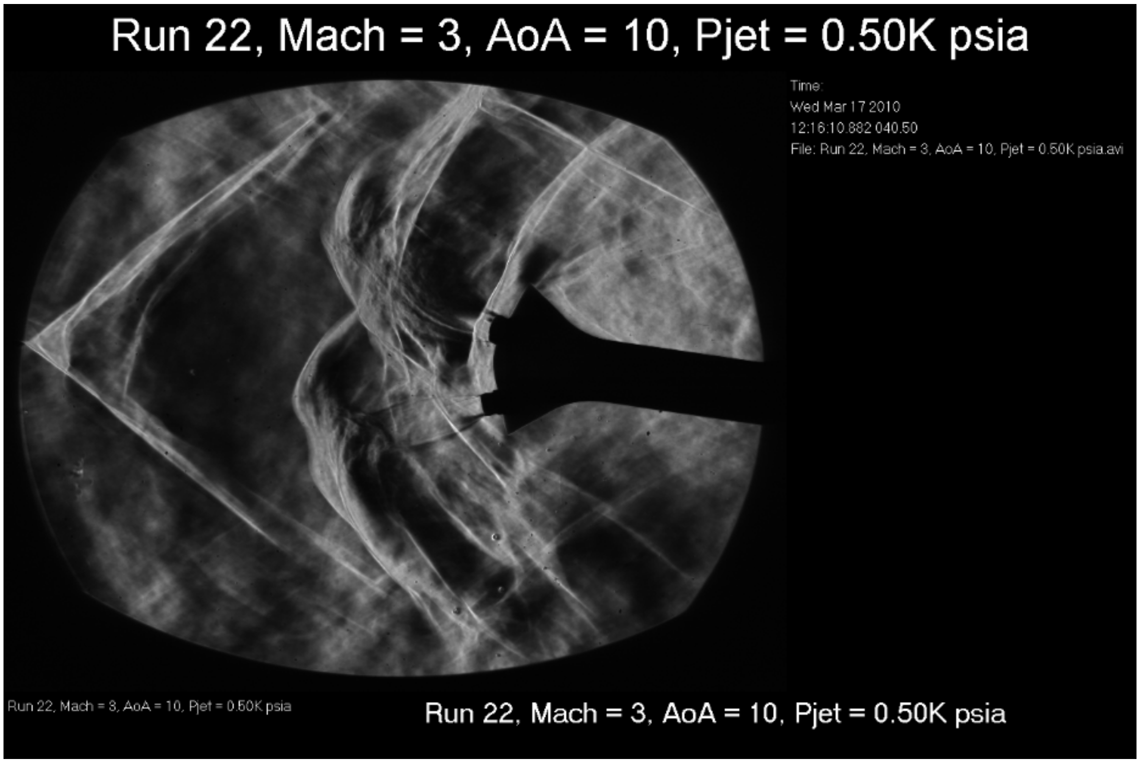

Figure A.9.—Schlieren image from 1x1 SWT testing—three engine model, Mach = 3.0, Re/ft = 1.44×10^6, and P_{total} (psi) = 8.66, AoA = 10°, 500 psia engine chamber pressure, tunnel unstart.

Figure A.10.—Schlieren image from 1x1 SWT testing—three engine model, Mach = 3.5, Re/ft = 1.86×10^6, and P_{total} (psi) = 15.00, AoA = 10°, 500 psia engine chamber pressure.

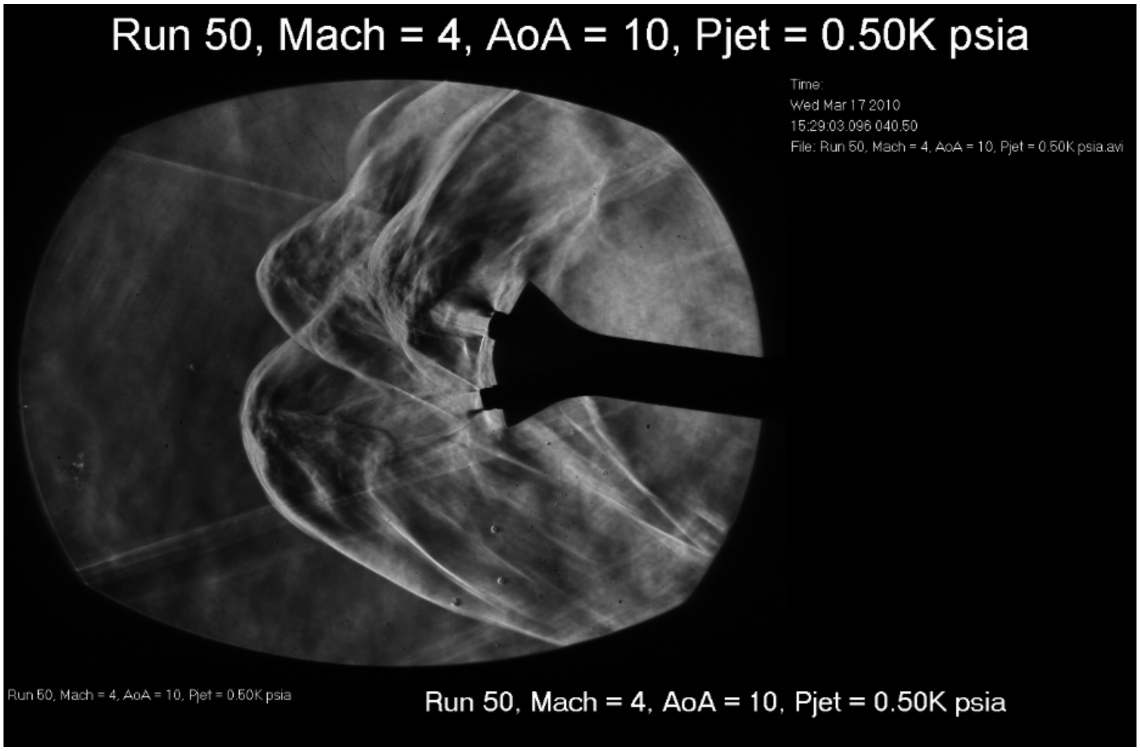

Figure A.11.—Schlieren image from 1x1 SWT testing—three engine model, Mach = 4.0, Re/ft = 2.56×10^6, and P_{total} (psi) = 26.01, AoA = 10°, 500 psia engine chamber pressure.

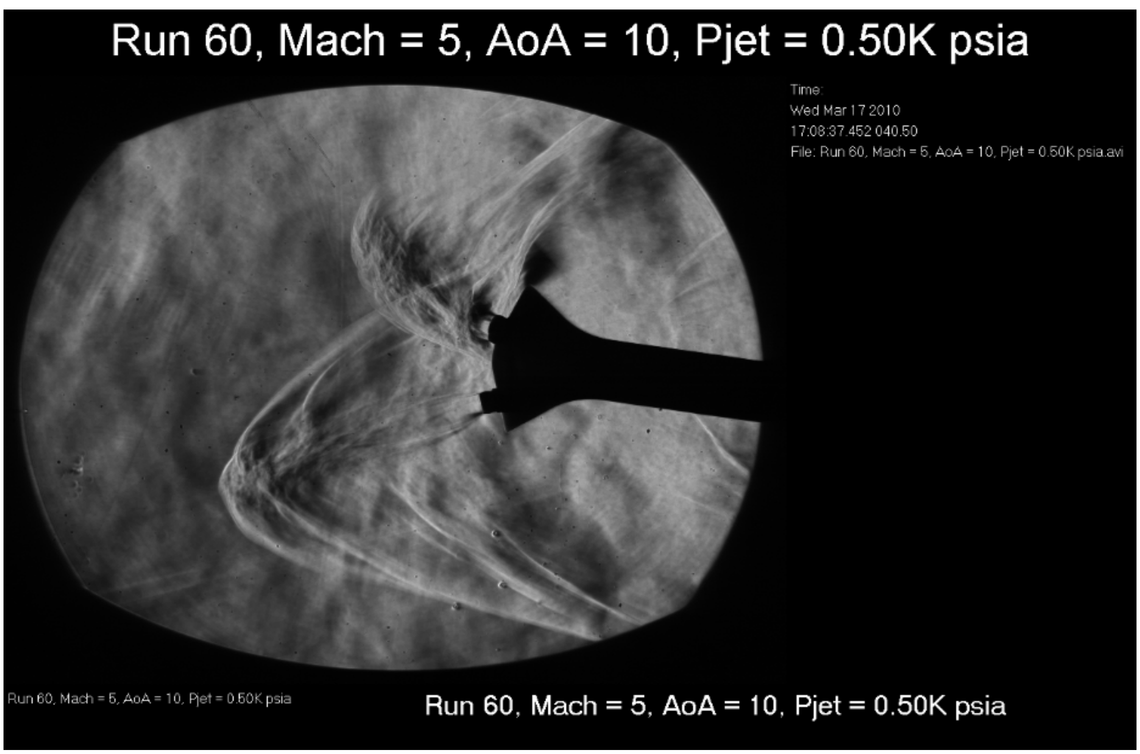

Figure A.12.—Schlieren image from 1x1 SWT testing—three engine model, Mach = 5.0, Re/ft = 5.42×10^6, and P_{total} (psi) = 90.40, AoA = 10°, 500 psia engine chamber pressure.

Appendix B.—SRP Run Data, 1×1 SWT

NASA EDL SRP 1×1 SWT TEST RESULTS SUMMARY, MARCH 17, 2010

Rdg	Scan	Total _sc	Navg	Date	Time	P_{total}, psia	P_{static}, psia	Mach number	Re/ft	P_{jet}, psia	AOA, deg.
6	1	1	0	17-Mar-10	10:05:08	5.10347	0.3425	2.41215	1.10×10^6	200	0
7	1	1	0	17-Mar-10	10:15:37	5.00908	0.335	2.41438	1.08×10^6	200	10
8	1	1	0	17-Mar-10	10:23:10	5.05017	0.335	2.41961	1.08×10^6	300	10
9	1	1	0	17-Mar-10	10:34:14	4.98458	0.3305	2.4199	1.07×10^6	300	0
10	1	1	0	17-Mar-10	10:40:37	5.02854	0.333	2.4207	1.08×10^6	500	0
11	1	1	0	17-Mar-10	10:47:04	4.98026	0.3285	2.42324	1.07×10^6	500	10
16	1	1	0	17-Mar-10	11:28:13	8.5857	0.2705	2.90301	1.44×10^6	200	10
17	1	1	0	17-Mar-10	11:41:31	8.44954	0.2655	2.90478	1.41×10^6	200	10
18	1	1	0	17-Mar-10	11:47:55	8.44737	0.265	2.90585	1.41×10^6		
19	1	1	0	17-Mar-10	11:51:28	8.47748	0.2655	2.90696	1.41×10^6	200	0
20	1	1	0	17-Mar-10	11:58:26	8.66597	0.271	2.90794	1.45×10^6	300	0
21	1	1	0	17-Mar-10	12:07:46	8.49397	0.266	2.907	1.42×10^6	300	10
22	1	1	0	17-Mar-10	12:15:42	8.66238	0.2695	2.91134	1.44×10^6	500	10
23	1	1	0	17-Mar-10	12:22:04	8.94823	0.285	2.89584	1.50×10^6	500	0
30	1	1	0	17-Mar-10	13:17:15	14.9783	0.207	3.46295	1.88×10^6	200	0
33	1	1	0	17-Mar-10	13:36:17	15.0123	0.205	3.47135	1.87×10^6	200	10
34	1	1	0	17-Mar-10	13:37:19	15.0393	0.205	3.47261	1.87×10^6	300	10
35	1	1	0	17-Mar-10	13:43:25	15.0024	0.2025	3.4795	1.86×10^6	300	0
36	1	1	0	17-Mar-10	13:49:28	15.0258	0.203	3.47887	1.87×10^6	300	15
37	1	1	0	17-Mar-10	13:55:21	14.8584	0.201	3.47795	1.85×10^6	500	15
38	1	1	0	17-Mar-10	14:01:20	15.0031	0.203	3.4778	1.86×10^6	500	10
39	1	1	0	17-Mar-10	14:07:15	15.0038	0.1985	3.49359	1.85×10^6	500	0
43	1	1	0	17-Mar-10	14:46:17	25.8632	0.1825	3.94839	2.55×10^6	200	0
44	1	1	0	17-Mar-10	14:52:20	26.8485	0.1915	3.94039	2.66×10^6	200	10
45	1	1	0	17-Mar-10	15:00:02	26.1978	0.1845	3.94985	2.58×10^6	200	15
46	1	1	0	17-Mar-10	15:05:52	26.3128	0.1875	3.9411	2.61×10^6	300	15
47	1	1	0	17-Mar-10	15:11:27	25.9392	0.185	3.94045	2.57×10^6	300	10
48	1	1	0	17-Mar-10	15:17:25	26.1281	0.185	3.94585	2.58×10^6	300	0
49	1	1	0	17-Mar-10	15:23:23	26.3289	0.1855	3.94954	2.60×10^6	500	0
50	1	1	0	17-Mar-10	15:29:02	26.0068	0.182	3.95456	2.56×10^6	500	10
51	1	1	0	17-Mar-10	15:34:48	26.7106	0.187	3.95427	2.63×10^6	500	15
57	1	1	0	17-Mar-10	16:48:45	86.9416	0.176	4.94131	5.54×10^6	200	15
58	1	1	0	17-Mar-10	16:56:23	90.1885	0.1675	5.01495	5.58×10^6	300	15
59	1	1	0	17-Mar-10	17:02:19	89.7116	0.161	5.04444	5.48×10^6	500	15
60	1	1	0	17-Mar-10	17:08:35	90.403	0.1535	5.09235	5.42×10^6	500	10
61	1	1	0	17-Mar-10	17:15:12	90.3647	0.1455	5.13857	5.32×10^6	300	10
62	1	1	0	17-Mar-10	17:21:26	90.4469	0.14	5.17308	5.25×10^6	200	10
63	1	1	0	17-Mar-10	17:27:29	90.0932	0.1325	5.21807	5.14×10^6	200	0
64	1	1	0	17-Mar-10	17:33:12	92.3942	0.13	5.25723	5.19×10^6	300	0
65	1	1	0	17-Mar-10	17:39:16	89.3562	0.118	5.31368	4.91×10^6	500	0

Appendix C.—Model Drawing, Front (Windward) of the Aeroshell

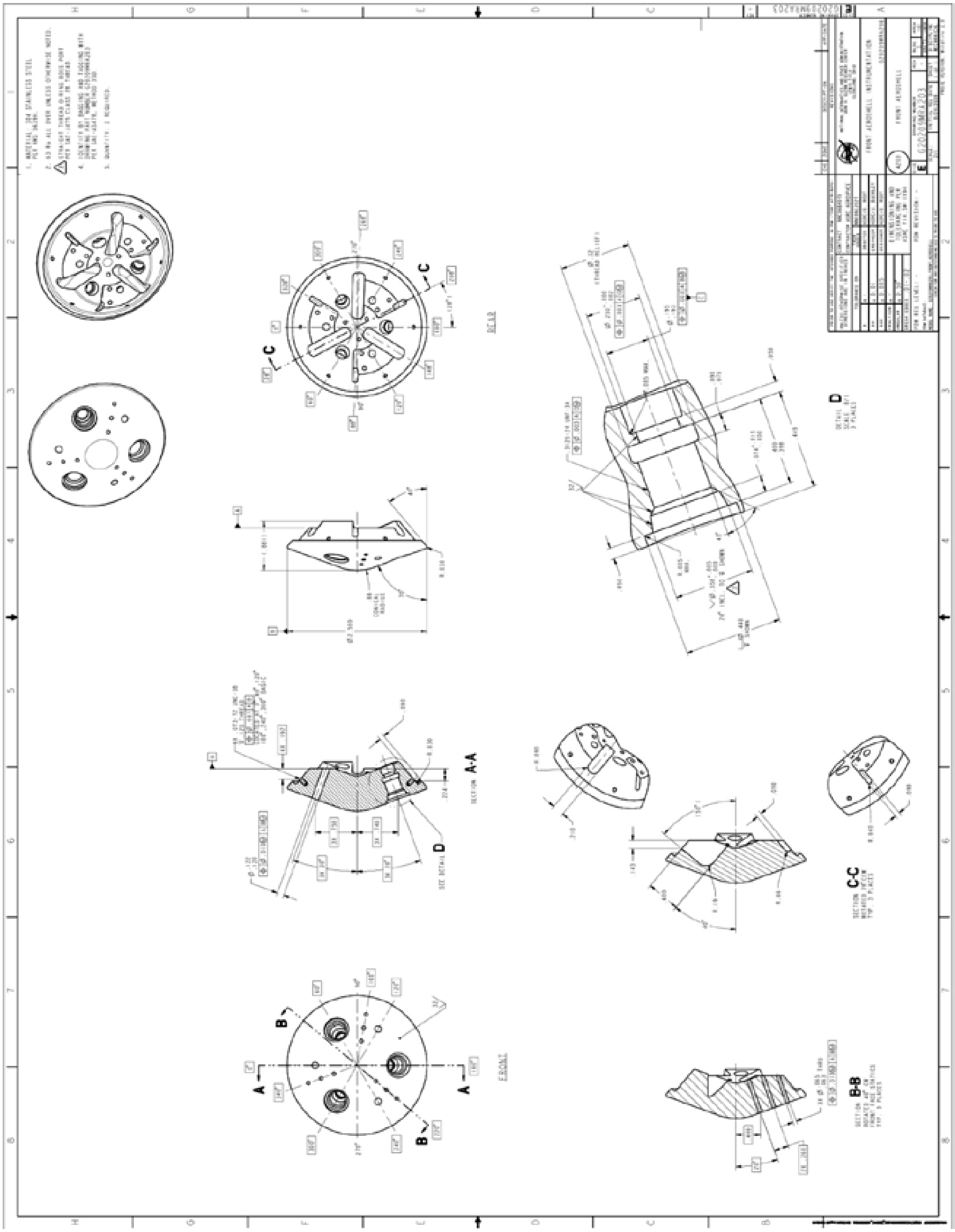

References

Entry, Descent, and Landing:

1. Karl T. Edquist, Artem A. Dyakonov, Michael J. Wright, and Chun Y. Tang, "Aerothermodynamic Environments Definition for the Mars Science Laboratory Entry Capsule," AIAA 2007-1206, 45th AIAA Aerospace Sciences Meeting and Exhibit, Reno, NV, 8 - 11 January 2007.
2. Karl T. Edquist and Stephen J. Alter, "Computational Aeroheating Predictions for Mars Lander Configurations," AIAA 2003-3639, 36th AIAA Thermophysics Conference, Orlando, FL, 23-26 June 2003.
3. Philip O. Jarvinen and Richard H. Adams, "The Aerodynamic Characteristics of Large Angled Cones with Retrorockets: Final Report," Contract No. NAS 7-576, Prepared by MITHRAS, Report number MC 70 - 3001 - R2 (BNY), February 1970.

Mars:

4. Palaszewski, B., Frisbee, R., "Advanced Propulsion for the Mars Rover Sample Return Mission," AIAA PAPER 88-2900, Jul 01, 1988.
5. Hepp, Aloysius F., Linne, Diane L., Landis, Geoffrey A., Groth, Mary F. Colvin, James E., "Production and Use of Metals and Oxygen for Lunar Propulsion," NASA-TM-105195, AIAA Paper 91-3481, Jan 01, 1991.
6. Linne, Diane L., and Meyer, Michael L., "Technical prospects for utilizing extraterrestrial propellants for space exploration," NASA-TM-105263 presented at the 42nd International Astronautical Congress, Montreal, Quebec, 5-11 Oct. 1991; sponsored by International Astronautical Federation International Astronautical Congress Montreal, Quebec, 5-11 Oct. 1991.
7. Rice, E., "Final Report On Advanced System Concept For Total ISRU Based Propulsion And Power Systems For Unmanned And Manned Mars Exploration" Orbital Technologies Corporation, National Institute for Advanced Concepts (NIAC) Phase II Contract, Research Grant 07600-041, OTC-GS-0096-FR-2002-1, Universities Space Research Association (USRA), 30 April 2002. Also, see: http://www.niac.usra.edu/files/studies/final_report/pdf/395Rice.pdf
8. Drake, Bret (editor), "Human Exploration of Mars Design Reference Architecture 5.0." NASA SP-2009-566, July 2009.

Alternate Retropropulsion Configurations and Vehicle Stability Options:

9. Putnam, L. and Capone, F., "Experimental Determination of Equivalent Solid Bodies to Represent Jets Exhausting into a Mach 2.20 External Stream," NASA TN-D-5553, December 1969.
10. Olen P. Fly and Robert W. Hockenberger, "Rocket Exhaust Effects on Radio Frequency Transmission," J. or Spacecrafts and Rockets, Vol. 3, pp. 310-314, 1966.
11. Anon., "NASA KSC/AFRL Reusable Booster System (RBS) Concept of Operations (ConOps)," RBS ConOps Study Team Kennedy Space Center, FL, December 7, 2010.
12. Barry M. Hellman, Dr. Scott E. Sherer, Christopher R. Schrock, Brock J. Pleiman, Anthony J. Piplic, and Dr. Brad St. Germain "Critical Flight Conditions of Operational Rocketback Trajectories," AIAA SPACE 2012 Conference & Exposition, AIAA 2012-5208, September 2012.
13. James DeSpirito, Harris L. Edge, Paul Weinacht, Jubaraj Sahu, and Surya Dinavahi, "Computational Fluid Dynamic (CFD) Analysis of a Generic Missile With Grid Fins," ARL-TR-2318, September 2000.
14. K. Mohamed Bak, "Experimental Investigation and Computational Fluid Dynamics Analysis of Missile With Grid Fin in Subsonic Flow," International Journal of Engineering Science and Technology, Vol. 2(11), 2010, 6214-6220.
15. Philippe Reynier, Uwe Reisch, José-Maria Longo, Rolf Radespiel, "Flow predictions around a missile with lattice wings using the actuator disc concept," Aerospace Science and Technology, Vol. 8, Issue 5, July 2004, pp. 377-388.

16. Despirito, J., Vaughn, M., Washington, W.D. “CFD investigation of canard controlled missile with planar and grid fins in supersonic flow,” AIAA Paper 2002-4509, August 2002.
17. Gregg Abate, Gerald Winchenbach, and Wayne Hathaway, “Transonic Aerodynamic and Scaling Issues for Lattice Fin Projectiles tested in a Ballistics Range,” 19th International Symposium of Ballistics, 7-11 May 2001, Interlaken, Switzerland.
18. James Despirito, Harris L. Edge, Paul Weinacht and Juburaj Sahu. “CFD Analysis of Grid for Maneuvering Missiles” AIAA 2000-0391.
19. E.Y. Fournier, “Wind tunnel investigation of a high L/D projectile with grid fin and conventional planar control surfaces,” 19th International Symposium of Ballistics, 7-11 May 2001, Interlaken, Switzerland.
20. John E. Burkhalter, Roy J. Hartfield, and Todd M. Leleux “Nonlinear Aerodynamic Analysis of Grid Fin Configurations” Journal of Aircraft, Vol. 32, No. 3, May - June 1995.
21. Ross A. Brooks and John E. Burk halter “Experimental and Analytical Analysis of Grid Fin Configurations” Journal of Aircraft, Vol. 26, No. 9, September1989.
22. John E. Burkhalter and Harris M. Frank “Grid Fin Aerodynamics for Missile Applications in Subsonic Flow,” Journal of Spacecraft and Rockets. Vol. 33, No.1 Jan – Feb 1996.
23. Andrews, Dana, “Design Optimization of High Mass Mars Entry Systems,” Paper Number IAC-08.D2.3.8 Andrews Space & Technology, 2008.

The Outer Planets:

24. Powell, Paniagua, Maise, Ludewig, Todosow Exploration of Jovian Atmosphere Using Nuclear Ramjet Flyer, IAF 98-S.6.08, PUR-4, 24 July 1998. Also, see: http://www.newworlds.com/reports/PUR-4.PDF
25. John Paniagua, James R. Powell and George Maise, “Europa Sample Return Mission Utilizing High Specific Impulse Propulsion Refueled with Indigenous Resources,” Report No. PUR. 21, Phase I. Final Report, Plus Ultra Technologies, Inc., National Institute for Advanced Concepts (NIAC) Phase I Grant 07600-077, Prime Contract Number NAS5-98051, November 30, 2001. Also see: http://www.niac.usra.edu/files/studies/final_report/pdf/638Paniagua.pdf
26. V.I. Shematovich and R.E. Johnson, “Near-Surface Oxygen Atmosphere at Europa,” Adv. Space Res. Vol. 27, No. 11, pp. 1881-1888, 2001, Pergamon Press, © 2001 COSPAR. Published by Elsevier Science Ltd., Printed in Great Britain.
27. Christopher F. Chyba and Cynthia B. Phillips, “Possible ecosystems and the search for life on Europa,” PERSPECTIVE, Proceedings of the National Academy of Sciences (PNAS), USA, January 30, 2001, vol. 98, no. 3, pp. 801–804.
28. Thomas B. McCord, Gary B. Hansen, and Charles A. Hibbitts, “Hydrated Salt Minerals on Ganymede's Surface: Evidence of an Ocean Below,” Science, 2001 May 25; 292: 1523-1525.
29. T. B. McCord, R. W. Carlson, W. D. Smythe, G. B. Hansen, R. N. Clark, C. A. Hibbitts, F. P. Fanale, J. C. Granahan, M. Segura, D. L. Matson, T. V. Johnson, and P. D. Martin, “Organics and Other Molecules in the Surfaces of Callisto and Ganymede,” Science, 1997 October 10; 278: 271-275.
30. Adam P. Showman and Renu Malhotra, “The Galilean Satellites,” Science 1999 October 1; 286: 77-84.
31. R. Carlson, W. Smythe, K. Baines, E. Barbinis, K. Becker, R. Burns, S. Calcutt, W. Calvin, R. Clark, G. Danielson, A. Davies, P. Drossart, T. Encrenaz, F. Fanale, J. Granahan, G. Hansen, P. Herrera, C. Hibbitts, J. Hui, P. Irwin, T. Johnson, L. Kamp, H. Kieffer, F. Leader, E. Lellouch, R. Lopes-Gautier, D. Matson, T. McCord, R. Mehlman, A. Ocampo, G. Orton, M. Roos-Serote, M. Segura, J. Shirley, L. Soderblom, A. Stevenson, F. Taylor, J. Torson, A. Weir, and P. Weissman, “Near-Infrared Spectroscopy and Spectral Mapping of Jupiter and the Galilean Satellites: Results from Galileo's Initial Orbit,” Science, 1996 October 18; 274: 385-388.
32. R. W. Carlson, M. S. Anderson, R. E. Johnson, W. D. Smythe, A. R. Hendrix, C. A. Barth, L. A. Soderblom, G. B. Hansen, T. B. McCord, J. B. Dalton, R. N. Clark, J. H. Shirley, A. C. Ocampo, and D. L. Matson, “Hydrogen Peroxide on the Surface of Europa,” Science 1999 March 26; 283: 2062-2064.

33. Amanda E. Lowell, Kah-Siew Ho, and Robert A. Lodder, “Remote Hyperspectral Imaging of Endolithic Biofilms Using a Robotic Probe,” Contact in Context:v1i1/planetprobe, Copyright 2002 Contact in Context. This article is available at http://cic.setileague.org/v1i1/planetprobe.pdf
34. Frank D. Carsey, Gun-Shing Chen, James Cutts, Lloyd French, Roger Kern, A., Lonne Lane, Paul Stolorz, and Wayne Zimmerman, and Phil Ballou Exploring Europa’s Ocean: A Challenge For Marine Technology Of This Century,” JPL 00-0221, Marine Technology Society Journal, Deep Ocean Frontiers Issue, Washington D.C., USA, 2000. http://techreports.jpl.nasa.gov/2000/00-0221.pdf
35. David F. Woerner, “Revolutionary Systems And Technologies For Missions To The Outer Planets,” Advanced Scientific Space Missions, Aosta, Italy, June 29-July 1, 1998. http://techreports.jpl.nasa.gov/1998/98-0522.pdf
36. Palaszewski, B., “Atmospheric Mining in the Outer Solar System: Mission Scenarios and Options For In-Situ Resource Utilization,” AIAA 2007-5598, July 2007.
37. Palaszewski, B., “Atmospheric Mining in the Outer Solar System: Vehicle Design Issues,” AIAA 2006-5222, July 2006.
38. Palaszewski, B., “Atmospheric Mining in the Outer Solar System,” AIAA 2005-4319, July 2005.
39. Andrews, D. G. (Boeing Co., Seattle, WA.) Bloetscher, F. (Goodyear Aerospace Corp., Akron, OH), “Aerobraked Orbital Transfer Vehicle Definition,” AIAA-1981-279, January 1981, 9 p.
40. R. Dyke, Swales Aerospace, Hampton, VA, and G. Hrinda, NASA Langley Research Center, Hampton, VA, “ Structural Design For A Neptune Aerocapture Mission,” AIAA-2004-5179, August 2004.

REPORT DOCUMENTATION PAGE					*Form Approved* *OMB No. 0704-0188*
The public reporting burden for this collection of information is estimated to average 1 hour per response, including the time for reviewing instructions, searching existing data sources, gathering and maintaining the data needed, and completing and reviewing the collection of information. Send comments regarding this burden estimate or any other aspect of this collection of information, including suggestions for reducing this burden, to Department of Defense, Washington Headquarters Services, Directorate for Information Operations and Reports (0704-0188), 1215 Jefferson Davis Highway, Suite 1204, Arlington, VA 22202-4302. Respondents should be aware that notwithstanding any other provision of law, no person shall be subject to any penalty for failing to comply with a collection of information if it does not display a currently valid OMB control number. PLEASE DO NOT RETURN YOUR FORM TO THE ABOVE ADDRESS.					
1. REPORT DATE *(DD-MM-YYYY)* 01-09-2014		**2. REPORT TYPE** Technical Memorandum			**3. DATES COVERED** *(From - To)*
4. TITLE AND SUBTITLE Entry, Descent, and Landing with Propulsive Deceleration: Supersonic Retropropulsion Wind Tunnel Testing and Shock Phenomena					**5a. CONTRACT NUMBER**
					5b. GRANT NUMBER
					5c. PROGRAM ELEMENT NUMBER
6. AUTHOR(S) Palaszewski, Bryan					**5d. PROJECT NUMBER**
					5e. TASK NUMBER
					5f. WORK UNIT NUMBER WBS 475122.02.03.06.01
7. PERFORMING ORGANIZATION NAME(S) AND ADDRESS(ES) National Aeronautics and Space Administration John H. Glenn Research Center at Lewis Field Cleveland, Ohio 44135-3191					**8. PERFORMING ORGANIZATION REPORT NUMBER** E-18702
9. SPONSORING/MONITORING AGENCY NAME(S) AND ADDRESS(ES) National Aeronautics and Space Administration Washington, DC 20546-0001					**10. SPONSORING/MONITOR'S ACRONYM(S)** NASA
					11. SPONSORING/MONITORING REPORT NUMBER NASA/TM-2014-217891
12. DISTRIBUTION/AVAILABILITY STATEMENT Unclassified-Unlimited Subject Categories: 01, 20, 34, and 91 Available electronically at http://www.sti.nasa.gov This publication is available from the NASA Center for AeroSpace Information, 443-757-5802					
13. SUPPLEMENTARY NOTES Prepared for the 51st Aerospace Sciences Meeting, sponsored by the American Institute of Aeronautics and Astronautics, Grapevine, Texas, January 7–10, 2013.					
14. ABSTRACT The future exploration of the Solar System will require innovations in transportation and the use of entry, descent, and landing (EDL) systems at many planetary landing sites. The cost of space missions has always been prohibitive, and using the natural planetary and planet’s moon atmospheres for entry, and descent can reduce the cost, mass, and complexity of these missions. This paper will describe some of the EDL ideas for planetary entry and survey the overall technologies for EDL that may be attractive for future Solar System missions. Future EDL systems may include an inflatable decelerator for the initial atmospheric entry and an additional supersonic retropropulsion (SRP) rocket system for the final soft landing. A three engine retropropulsion configuration with a 2.5 in. diameter sphere-cone aeroshell model was tested in the NASA Glenn Research Center’s 1- by 1-ft 1×1 Supersonic Wind Tunnel (SWT). The testing was conducted to identify potential blockage issues in the tunnel, and visualize the rocket flow and shock interactions during supersonic and hypersonic entry conditions. Earlier experimental testing of a 70° Viking-like (sphere-cone) aeroshell was conducted as a baseline for testing of a SRP system. This baseline testing defined the flow field around the aeroshell and from this comparative baseline data, retropropulsion options will be assessed. Images and analyses from the SWT testing with 300- and 500-psia rocket engine chamber pressures are presented here. In addition, special topics of electromagnetic interference with retropropulsion induced shock waves and retropropulsion for Earth launched booster recovery are also addressed.					
15. SUBJECT TERMS Planetary entry; Propulsion; Rocket engines; Fluid mechanics; Retrorockets; In situ resource utilization; Retropropulsion					
16. SECURITY CLASSIFICATION OF:			**17. LIMITATION OF ABSTRACT**	**18. NUMBER OF PAGES**	**19a. NAME OF RESPONSIBLE PERSON** STI Help Desk (email:help@sti.nasa.gov)
a. REPORT U	**b. ABSTRACT** U	**c. THIS PAGE** U	UU	34	**19b. TELEPHONE NUMBER** ***(include area code)*** 443-757-5802